Fakultät für Medizin

Application of preoperative function-based structural connectome analysis combined with supervised machine learning to predict surgery-related language deficits after glioma resection

Dr. med. Haosu Zhang

Vollständiger Abdruck der von der Fakultät für Medizin der Technischen Universität München zur Erlangung des akademischen Grades eines

Doctor of Philosophy (Ph.D.)

genehmigten Dissertation.

Vorsitzende: Prof. Dr. Agnes Görlach
Betreuer: Prof. Dr. Sandro M. Krieg
Prüfende/-r der Dissertation:
1. Priv. -Doz. Dr. Christian Sorg
2. Prof. Dr. Prof. h.c. Florian Heinen

Die Dissertation wurde am 27.06.2022 bei der Fakultät für Medizin der Technischen Universität München eingereicht und durch die Fakultät für Medizin am 13.09.2022 angenommen.

für

Freiheit und Frieden

Danksagung

Seit ich 2017 zum Studium ans Klinikum rechts der Isar der TUM gekommen bin, war ich immer stolz darauf. Eine Prüfung nach der anderen, eine Herausforderung nach der anderen hat mich motiviert, mein Wissen zu erweitern.

Zunächst möchte ich mich bei meinem Doktorvater, Prof. Dr. med. Sandro Krieg, für die Chance bedanken, in seiner Arbeitsgruppe am Klinikum rechts der Isar zu promovieren. Mit seiner ständigen Anleitung und Unterstützung habe ich nicht nur mein medizinisches Wissen erweitert, sondern auch zahlreiche wichtige Erfahrungen für zukünftige Arbeit und Forschung gesammelt. Außerdem habe ich gelernt, dass es in der Medizin auch um Humanität geht und nicht nur um Geräte und Daten.

Ich möchte auch meinen Mentor PD Dr. med. Sebastian Ille danken. Er unterstützt mich stets bei meinen Ideen und ist mir bei der Durchführung meiner Projekte eine große Hilfe. Er unterstützt mich stets bei meinen Ideen und ist mir bei der Durchführung meiner Projekte eine große Hilfe. Ich bekomme von ihm immer klare Hinweise und neue Einsichten, wenn ich ein schwieriges Problem zu bewältigen haben muss.

Ich möchte meinen Eltern (Shuyi Cao und Weiming Zhang) und meiner Familie für ihre Ermutigung und Unterstützung beim Auslandsstudium danken. Ihre aufgeschlossene und fortschrittliche Meinung hat mich tief beeinflusst. Sie haben mich gelehrt, fleißig zu lernen und unabhängig zu denken. Ich vermisse meine Großmutter und meinen Großvater.

Darüber hinaus möchte ich meinen Freunden Axel, Marc, Severin, Ann-Katrin, Leonie, Beaten und Enrik, die auch meine Kollegen sind, meinen herzlichen Dank aussprechen. Sie haben mir in meinem Leben und Studium sehr geholfen und ließen mich die Schönheit und Freundlichkeit in Deutschland empfinden.

TABLE OF CONTENTS

1. ABBREVIATION

3D	Three-Dimensional
AD	Average Degree
ADM	Abductor Digiti Minimi
AL	Average shortest path Length
APB	Abductor Pollicis Brevis
BMRC	British Medical Research Council
BOLD-fMRI	Blood Oxygen Dependent - Functional Magnetic Resonance Imaging
DES	Direct Electrical Stimulation
DICOM	Digital Imaging and Communications in Medicine
DTI	Diffusion Tensor Imaging
EEG	Electroencephalography
EG	Global Efficiency
EL	Local Efficiency
FA	Fractional Anisotropy
FAT	Fractional Anisotropy Threshold
FAR	Fractional Anisotropy Ratio
FCR	Flexor Carpi Radialis
FLAIR	Fluid-attenuated Inversion Recovery
FT	Fiber Tracking
IFG-oper	opercular part of Inferior Frontal Gyrus
IFG-tria	triangular part of Inferior Frontal Gyrus
IPG	Inferior Parietal Gyrus
ITG	Inferior Temporal Gyrus
GTR	Gross Total Resection
MEG	Magnetoencephalography

MEP	Motor Evoked Potential
MTG	Middle Frontal Gyrus
MOG	Middle Occipital Gyrus
mSFG	medial Superior Frontal Gyrus
MTG	Middle Temporal Gyrus
NA	No Aphasia
nTMS	navigated Transcranial Magnetic Stimulation
ONT	Object Naming Task
PosG	Postcentral Gyrus
PreG	Precentral Gyrus
rMT	resting Motor Threshold
SFG	Superior Frontal Gyrus
SMA	Supplementary Motor Area
SmG	Supramarginal Gyrus
SOG	Superior Occipital Gyrus
SPG	Superior Parietal Gyrus
SRA	Surgery Related Aphasia
TP	Temporal Pole

2. INTRODUCTION

2.1 Language Function and Glioma Resection

2.1.1 Tumore-related Language Deficits

In a previous study, the incidence of glioma was found at 5.60 (5.56 ~ 5.65) per 100,000 person-years, whereas the incidence of glioblastoma was reported at 2.99 (2.96 ~ 3.02) per 100,000 person-years in the USA (Lin *et al.*, 2021), and with an age-adjusting incidence rate up to 3.22 per 100,000 population, accounting for 57.3 percent of total gliomas cases and 48.3 percent of all malignant intracranial tumors (Ostrom *et al.*, 2019).

Glioma growth in the brain is not only an invasion of tissue structure but also has a significant impact on brain function. Currently, many studies on brain function under the impacts of cerebral tumors have focused on motor and language, and the inherent complexity of the latter has led to challenges in research, which has attracted a great deal of academic attention and effort. Patients with brain tumors can manifest various language-related symptoms, often termed clinically as spoken language disorder, or oral language disorder, including phonology, morphology, syntax, semantics, pragmatics, and so on. In clinical practice, it is often difficult to subdivide the different language-related manifestations. They are usually categorized according to symptoms, including motor aphasia, reading aphasia, etc.; In addition, they are graded according to the symptomatic severity. This eliminates the burden of analyzing the complicated structures of language itself and allows better focus on the tumor, the main object of treatment.

Certainly, in many cases, the degree of functional impairment is related to the extent of tumor invasion and its growth rate. However, what is noteworthy in clinical practice is that many patients' symptoms are not as corresponding to tumor properties as described previously in the conventional anatomy. These phenomena led to such kinds of tumor can be majorly categorized into the following two aspects: firstly, the tumor is large, but the pathological signs and symptoms found in the patient's physical examination or from the patient's self-reported complaints are not serious; secondly, there is a mismatch between the patient's functional deficits and the regional cerebral function corresponding to the location of the tumor. It is worth thinking about the appearance of

these contradictions. Furthermore, the diversity that already characterizes human beings' languages, such as different kinds and structures of language and expressions of thoughts, also leads to the complexity in investigations regarding differences and similarities among the various linguistic modalities and their relationship with brain structures. This renders the clarification of the triangle relationship between the different modalities of language, cerebral language function, and their corresponding structures becoming even more complicated.

Many researchers have explored and proposed various hypotheses to explain the relationship between cerebral regions and language functions so that to explain the phenomenon contrary to the understandings of functional organizations based on classical functional anatomy. Currently, the more accepted ideas among them are functional plasticity, functional reorganization, and functional brain networks. It is evident that these hypotheses challenge the traditional functional anatomical view that " a one-to-one correspondence between cerebral function and structure" by focusing on the dynamic relationship between cerebral function and regions and emphasizing the importance of their interactions and collaboration during functional processing. This can enable us to further understand the variable signs and symptoms caused by tumors, furthermore, enhance the view regarding the brain as a balanced functional entity.

2.1.2 Surgery Related Aphasia

Nowadays, although medical technology is advancing and treatments are constantly being updated, surgical resection is still regarded as the most important and effective aspect in treating gliomas. Nevertheless, we need to recognize that there are risks of postoperative sequelae associated with the surgical treatment, among which surgery related aphasia (SRA) is one of the most important ones. It is often assumed that resecting glioma in the vicinity of the eloquent areas of the language, especially within left-sided perisylvian regions, is likely to result in SRA, and such procedures are considered to be highly risky (Negwer *et al.*, 2018; Sollmann *et al.*, 2019).

In clinical practice, neurosurgeons encountered patients who have developed SRA after undergoing glioma resection, although the surgical areas did not reach brain areas regarded to be related to language functions; or vice-versa, after receiving surgery within language eloquent areas, the patient did not develop language deficits as preoperatively predicted. This uncertainty also implicates the insufficiencies when using

the traditional classical functional anatomy-based approach to empirically assess the surgery risk and functional prognosis. It is difficult to make predictions about postoperative functional alterations at the individual level. This suggests that the current assessments of the cerebral functional distribution and surgery risk evaluations do not fully meet the needs of contemporary individualized medicine. One of the challenges resides in defining which brain structures can be surgically removed with minimal interference to function. Hence, the development of new techniques and protocols to enable individualized assessments on the risk of resection extension is an urgent topic to be explored and researched, so that the critical regions can be identified then to be protected.

Defining the levels of involvement for each cerebral region regarding the performance of language functions aimed at providing an individualized assessment on postoperative risks of functional deficits, allowing for the development of individualized surgical implementation plans, thereby greatly improving the safety of surgery, and reducing the incidence of SRA. It is commonly acknowledged that the balance between gross total resection (GTR) and the preservation of normal brain functioning must be carefully regulated in order to prevent severe drawbacks in patients' postoperative life (Young *et al.*, 2015; Ogunlade *et al.*, 2019). Thus, on the one hand, achieving maximum removal of gliomas, which is an important prognostic factor for a long-termed tumor-free life for these patients, and on the other hand, preserving the potential for patient's functional recovery after surgery. Sollmann et al. reported that, when the glioma is localized in eloquent regions, functional outcomes were variously observed defined by critical areas preserved during surgery (Sollmann *et al.*, 2020a). Similarly, recent findings on language organization refer more to the individual level analysis (Ardila *et al.*, 2016), contributing to the modern concept of individualized treatment and function-specific glioma resection. Keeping this in mind, identifying new biomarkers that might predict the probability of SRA prior to surgery is critical for improving treatment strategies as well as preserving language function while still attempting a gross complete resection.

2.2 Cerebral Network and Connectome

In the last decade, more and more researchers have introduced the theory of functional networks or connectomes into their studies on cerebral language functions. Currently, in these investigations within human neuroscience domain, the data required for

analysis were collected primarily through various imaging techniques, including Electroencephalograph (EEG), functional Magnetic Resonance Imaging (fMRI), and Diffusion-Weighted Magnetic Resonance Imaging (DWI or DW-MRI). They are grounded in different physical theories and applied different engineering solutions，which determine their respective application focuses and various workflows, thus reflecting different aspects of the brain's brain functions and organizations.

Firstly, networks based on EEG are to investigate the changing models through whole-brain electro-cortical events that represent synchronized functional processes at a comprehensive level, allowing analyses on brain dynamics with high temporal resolution (Seeber *et al.*, 2019; Seeber and Michel, 2021; Takarae *et al.*, 2022). In the study by Wolthuis et al., pre-operative EEG network characteristics were without differences between glioma patients and healthy controls (Wolthuis *et al.*, 2021). However, the presence of hubs and higher local and global functional connections in the EEG network were identified to be associated with poorer preoperative language performances in patients with glioma and indicated a prognosis of worse speeching function one year after tumor resection (Wolthuis *et al.*, 2021).

Secondly, resting-state and task-based fMRI is widely utilized for the detection and monitoring of various brain functions. The activations of brain neurons are indirectly defined through the quantification of altered signals through measuring the Blood-oxygen-level-dependent (BOLD) in brain tissues, thereby localizing the brain regions corresponding to specific functions and demonstrating the interrelationship between different brain areas during the functioning process. The components of brain function networks and their collaborative and counteracting relationships were inferred from the degree of positive and negative correlation of BOLD signal fluctuations between brain regions. The degree of positive and negative correlation of BOLD signal fluctuations between different brain regions was used to infer the components of brain function networks as well as their collaborative and counteracting interactions. Several studies have reported that the connectivity of default mode network (DMN) nodes in the left temporal and parietal lobes were decreased, which was related to the poor execution of language functions and the worse scores on tasks for assessing verbal working memory (Kocher *et al.*, 2020; Zoli *et al.*, 2021). Additionally, connectivity strengths in the left parietal DMN node were associated to working memory performance in both verbal and visual tasks (Kocher *et al.*, 2020; Zoli *et al.*, 2021).

Thirdly, the structural connections between different brain regions are concluded by performing fiber tracing in DWI images. This provides a visualization of subcortical structural connections between different cortical regions. Up to the date, it can be noted that unfortunately, only a few previous studies have covered the role of the structural network in language performance. Most of these studies focused on the number or volume of single or several tracts in the subcortical regions to analyze their relations with changes in neural function (Sollmann *et al.*, 2018a; Yuan *et al.*, 2020; Ille *et al.*, 2021), rather than at an integrated network level. Ille et al. investigated changes of single white matter pathways based on functionally mapped seeds via nTMS and indicated that they were correlated with their corresponding status of language function regarding the tracks consisting of frontal aslant tract, inferior fronto-occipital fascicle, superior longitudinal fascicle, and arcuate fascicle (Ille *et al.*, 2018).

Collectively, we can recognize the relationship between functional networks and the maintenance of language function in the brain from the studies of functional brain images. Various regions within the brain work cooperatively or adversely with each other to achieve a balanced and stable presentation of function. However, it is also not difficult to see that current research on structural networks lags far behind functional networks. It is well-known that the generation of functions relies on the structural basis and is not able to interact with each other when being without subcortical connections. We need to further explore the language-related cortical and subcortical structural networks to provide new insights into the dynamic changes of language, which is one of the research focuses of the current study.

2.3 Diffusion Tensor Images based Structural Connectome and Language Function

2.3.1 Diffusion Tensor Images based Structural Connectome

Diffusion tensor imaging (DTI), a subset of DWI, has been widely applied in clinical practice and neuroscientific research to visualize white matter tractography in the brain, producing images from the results of a comprehensive calculation on the diffusion of water molecules in different directions to generate contrast during MR scanning. In the tissue characterized by an internal fibrous structure similar to the anisotropy of certain crystals, such as the neuronal axons of white matter in the brain, water molecules will

subsequently move more freely along the direction aligned with the neural fiber (axial diffusion) and more limited in the direction perpendicular to the neural axon pathway (perpendicular diffusion, or radial diffusion). It is implied that the observed diffusion rates are vary depending on the directions. By applying magnetic fields in different directions to water molecules in the brain to interfere with their Brownian motion of water, the changes in their energy are obtained to determine the main direction based on the maximal movement of water molecules and thus generate contrast during MR imaging for the visualization of the subcortical neural pathways.

Previous DTI investigations, as mentioned above, have primarily focused on single or a few neural tracts rather than the brain network as a whole, which is insufficient for understanding the structural basis of functional alterations. As shown in the graph theory-based studies conducted by other institutes, their findings regarding the cerebral functional and structural organizations are compatible with the hypothesis that the cerebral evolution aimed to keep a dynamic balance between maximizing the efficiency in transferring information among regions and minimizing the energy cost for connections, so that to adjust the functional processing and output within the normal range (Bullmore and Sporns, 2009; Betzel et al., 2014; Gargouri et al., 2016). It is well documented that such organizational characteristics are observed in many fMRI and EEG studies. Meanwhile, it is worth noting that those functional-level studies did not provide a comprehensive and sufficient answer to the question “What are the connectome properties of the brain?”. Whether such kinds of changes in structural networks were also maintained through a similar dynamic homeostatic mechanism, furthermore, whether they have robustness or reorganization in response to external or internal pathological or physiological abnormalities has not been well elucidated, which is of great significance for the scope of protection in neurosurgical and radiological treatments. Drawing on our previous experience and that of other centers, challenges, or problems in conducting such analyses are mainly in two aspects, as followings:

Firstly, interindividual differences in brain volume are evident in both healthy controls and tumor patients. DTI techniques were based on voxel units and can-not eliminate the interference of such inter-individual differences for visualization of the tractography. The primary problem is on “How to counteract this interindividual variation?” which should be firstly addressed for further analysis.

Secondly, when applying DTI data for fiber tracking (FT) to reconstruct structural brain networks, different choices in parameters can lead to different results, mainly including fractional anisotropy (FA), fiber length (FL), and angular thresh-old (AT). Among them, the most critical one is the setup of the FA threshold, which varies considerably even among normal individuals, let alone in patients with brain tumors. Tumor-induced edema, hemorrhage, necrosis, and other pathological manifestations can interfere with the FT process. A single FA threshold, such as 0.15 or 0.10, is now rarely used in FT-related studies, also out of the same concern as ours. How to establish a more objective threshold setting is the second challenge to be faced in such studies.

2.3.2 Investigation of Structural Connectome

Aiming to fill this blank, we developed a new analysis protocol for studying function-related structural networks and applied it in an investigation of language performance in brain glioma patients from 2019 to 2021(Zhang *et al.*, 2021a). Since we cannot change the basic principle of the current DTI techniques for data acquisition, therefore, to improve the reliability of the analysis process in the algorithm to address the above two problems is our basic thought in developing the DTI structural network analysis protocol.

Firstly, previous studies have suggested the method of registering individual brains with template brains to eliminate structural differences between individuals. However, this process involved interpolation and other algorithms that may potentially change the original DTI data, which will lead to altered fiber tracking results in the registered data when compared with the original data. Regarding its application in glioma patients, this will result in even greater alterations due to structural deformation, edema, hemorrhage, etc. in lesion regions. Then it is necessary to alternatively think about how to balance the differences between individuals. Considering that the number of fibers itself is derived from voxel units, the connectome of cerebral connections is constructed by setting a threshold to binary the number of fibers to 1 (connected, above the thresh-old) and 0 (unconnected, below the thresh-old) between every two regions (Zhang et al., 2021a). We must admit that this does not completely eliminate interindividual differences, but it is the clearest and most straightforward algorithm that we can apply at the moment, without additional computational workload and with a significant increase

in processing speed. This is also in line with the principle of "directness and reliability" of the examination technique in the clinical context.

Secondly, differences in FA distribution between individuals have been reported in previous studies. Sollmann et al. adopted the threshold setting approach for fractional anisotropy threshold (FAT) in their DTI study, i.e., using 25%, 50%, and 75% of the highest individual FA values as thresholds (Sollmann *et al.*, 2020a). In our previous study protocol, we developed the visual ratio (VR) algorithm for setting FT thresholds (Zhang *et al.*, 2021a). The maximal FAT (FAT_{max}) in the brain and the maximal FA (fa_{max}) for every single fiber were identified during FT process, which is applied for calculating VR to define fibers (Zhang *et al.*, 2021a), which is same as the FAR in the current study. FAR derived from this FA-based numerical conversion can align the range of FA variations for different individuals to a percentage range, 0 ~ 100%, thus enabling a standardized metric obtained among individuals while maintaining the original quantitative characteristics of FA.

Through the two methods described above, we can be able to cope with the problems faced in previous DTI studies. Moreover, facilitated by those methods, the distribution of subcortical connections can be obtained, then construct structural matrices of connections between every two brain regions, thus realizing the connectome analysis of structural networks.

2.3.3 Connectome Measurements

In 2005, Sporns et al. suggested the term "connectome" referring to the organization consisting of functionally or anatomically segmented cerebral regions and their corresponding neural connections (Jonasson *et al.*, 2005; Sporns *et al.*, 2005; Wedeen *et al.*, 2005; Hanggi *et al.*, 2014). Subsequently, graph theory can be introduced in the neuroscience domain to investigate and intemperate the cerebral structural connectome (Henderson *et al.*, 2020; Mitsuhashi *et al.*, 2020; Arefin *et al.*, 2021). In the macroscale connectome generated from DTI, the nodes of this network (or graph) are the brain regions of interest (ROI), depending on the structural and functional parcellation templates, and the edges of the graph are derived from the axons interconnecting those areas, tracked by FT process. After that, the complex 3-dimensional brain regions and their connections are converted into a 2-dimensional diagonally symmetric matrix according to the previous analysis scheme (Jonasson *et al.*, 2005; Sporns *et al.*,

2005; Wedeen *et al.*, 2005; Hanggi *et al.*, 2014; Zhang *et al.*, 2021a). Thus, connectomes are turned into brain graphs because they are indeed the graphs according to the mathematical termination, describing the neural connections in the brain, so that graph theory parameters can be introduced to measure the brain network (Jonasson *et al.*, 2005; Sporns *et al.*, 2005; Wedeen *et al.*, 2005; Zhang *et al.*, 2021a).

Through the analysis based on the models generated from the nonlinear dynamics of ROIs and their interconnections, it resulted in patterns of statistical dependencies to present functional connections, and causal interactions to indicate the effective connections within the structural connectome derived from DTI, thus defining different major functional modalities of complex neural systems (Sporns and Kotter, 2004; Sporns *et al.*, 2005; Gollo and Breakspear, 2014). No matter how complex the models might be, the fundamental analysis of graph theory remained primarily at three levels: (1) node (functionally relevant brain regions), (2) edge (connections between ROIs), and (3) network (functional brain network composed of nodes and edges). For the implementation of structural connectivity in clinical applications, an initial step is to explore brain function from these three fundamental aspects.

Firstly, considering the context of the study on the cerebral language function, the main focus of the node analysis is on the brain regions related to language processing, and their similarities and differences within and between different individuals or groups. This furthermore is needed to investigate the organization of language functions in the cortical regions, which is corresponding to the network analysis at the nodal level. In previous studies, fMRI and EEG were preferred for those purposes. The correlation between certain regions and functions can be reflected by the alteration of the signal before and after the execution of the function.

Secondly, it is the investigation at the edge level regarding subcortical neural connections between different brain regions for their respective involvements in various functional performances. In contrast to previous studies, a connectomics study can not attribute the language function to the effect of one or a few cerebral tracts, but rather be based on a comprehensive analysis of the connections at network level. The commonly used measurements are: (1) Average degree (AD), it is one of the basic properties to represents the intensity of edges across all nodes in a specific network, which is hereby to assess the intranetwork strengths of neural connections between different cerebral regions (Cohen and D'Esposito, 2016); (2) Average shortest path length (AL)

is defined to be the average quantities of edges (or sum of edges weights) along the shortest pathway in a specific network or subnetwork regarding all its possible pair-wise-connected nodes (Seguin *et al.*, 2018), which is a metric used to assess the capacity of information or mass transmission at a network level (Jahanshad *et al.*, 2012). Those are to analyze the structural organization of nerve fibers that survive tumor interference.

Thirdly, there are many parameters at the network level that can be applied in the analysis of graph theory. Based on previous experience with structural brain connectomics (Sporns and Kotter, 2004; Sporns *et al.*, 2005; Gollo and Breakspear, 2014), the efficiency of a network is a measure of how efficiently it exchanges information, including global efficiency (EG) and local efficiency (EL): (1) The capacity of simultaneously transmission and processing of signals in a network is characterized by EG, calculated from the inverse of AL (Wang *et al.*, 2010), and higher EG represents more efficiently transferring parallel information in the net-work between nodes concurrently (Ratnarajah *et al.*, 2013); and (2) EL was determined by the global efficiency of a sub-network consisting of this node's neighborhood, aiming to measure how efficiently the information can be conveyed within the sub-network that is based on a particular node's neighboring nodes after removing this node (Wang *et al.*, 2010; Ratnarajah *et al.*, 2013), and it reflects the capacity of robustness in the sub-network, so as to show the effectiveness of the communication between the local node’s close neighboring nodes (Wang *et al.*, 2010). Measuring those efficiencies can improve the understanding of the mechanism of the functional performance, also corresponding to the findings in previous functional MRI-based studies.

By measuring these parameters, the basic properties and characteristics of the structural connectome can be assessed, allowing further analysis to elucidate the structural basis of producing cerebral function (Zhang *et al.*, 2021a). Regrettably, however, this study only considered functional performance in this single preoperative phase and no follow-up investigation on postoperative functional changes were conducted. There is still a research need to use these parameters based on graph theory to predict the postoperative language function prognosis.

2.4 Localization of Language Function

2.4.1 Navigated Transcranial Magnetic Stimulation

Through the above, it is evident that there are many areas involved in the analysis of brain structural networks from a whole-brain perspective alone, and it is still necessary to highlight the key cerebral areas associated with language function for a surgery consultation. To solve that problem, a variety of tools and methods have been developed and used to localize language function in brain regions. They all combine the language tasks and real-time brain signal acquisition techniques to record and monitor alterations in functional brain signals corresponding to abnormal performances during language tasks, such as fMRI combined with language tasks.

As mentioned previously, fMRI is susceptible to interference from confounding signals in the lesion areas when collecting cortical signals in glioma patients, and the resolution of EEG recordings is not sufficient to reach the requirements for surgical navigation. As mentioned previously, fMRI is susceptible to interference from mixed signals in the lesion areas when acquiring cortical signal changes in tumor patients, and the resolution of EEG signals to obtain neuronal potential signals in the brain is not sufficient to reach the level of surgical navigation. The motivation for seeking a device with more direct and high-resolution signals has been widely accepted and studied in neurosurgery in the last decade.

In fact, navigated transcranial magnetic stimulation (nTMS) is not only an electromagnetic stimulation technique, more exactly, but it is also a brain function interfering technique. Faraday's law of induction is an electromagnetism fundamental law that explains how a magnetic field would interact with an electric circuit to create an electromotive force, a process termed electromagnetic induction, which is the basic mechanism of nTMS. When the electric current passed through the copper coil in the nTMS coil, a magnetic field is generated. The phospholipid bilayer of the cell is a natural capacitor with the potential difference between inside and outside of the cell (Krieg *et al.*, 2017). If the magnetic field is large enough to induce a capacitive discharge, it will cause a potential change in the cell, such as depolarization and hyperpolarization, then a corresponding physiological effect can be elicited. The output intensity of nTMS stimulation is currently designed to be within the safe range and controllable, and its induced physiological reactions are only temporary, like a transient “*lesion*”, and will not cause long-term functional deficits or changes under guided applications (Krieg *et al.*, 2017).

Through nTMS it is possible for researchers or physicians to intervene in the execution of brain functions as if they were talking directly to the brain functions. This enables a direct clarification of the causal relationship between brain regions and alterations in language function.

By using the navigation technology, the high-resolution MRI T1-weighted image from the individuals was used as a 3-dimension roadmap for navigation, combined with the infrared ray tracking system on the stimulation coil, which can provide precise guidance for matching the aim of the nTMS stimuli to the predefined targets. Considering that the electric field refracts when passing through different densities of human tissues (scalp and skull), this can potentially lead to off-target stimulation output and thus cause misinterpretation. The most often utilized TMS navigating technique is electric field navigation, which can adjust the electric field position in real-time and then avoid off-target stimuli owing to electric field position offset. Compared to traditional linear navigation techniques, electric field navigation is more promising for neurosurgery, assisting clinicians accurately localizing function-relevant brain areas.

2.4.2 Reliability of nTMS for Language Localization

According to the guideline for nTMS language mapping, the stimuli were navigated to predefined targeted cerebral regions to induce language errors when patients conducting the object naming task. In this way, it is straightforward to identify the brain areas associated with language function.

Currently, the most widely adopted procedure in clinical practice for directly investigating brain function remains awake surgery, in which direct electrical stimulation (DES) testing and intraoperative neuro-monitoring (IONM) are systematically and routinely integrated. Despite the fact that several academics have highlighted out its limited applications and misconceptions in interpreting its results (Borchers *et al.*, 2011), it is still recognized as the most objective method, "gold standard", and used to assess the applicability and the reliability of other investigations in localizing the eloquent regions regarding specific functions (Talacchi *et al.*, 2013; Ottenhausen *et al.*, 2015). To guarantee the accuracy and precision of nTMS, its mapping findings associated with cerebral functional performance must therefore be compared to those of intraoperative DES testing (Talacchi *et al.*, 2013; Ille *et al.*, 2015b; Ottenhausen *et al.*, 2015). Dr. Ille et al. have been studying for many years in this domain and reported in 2015 that,

through comparisons of results between pre-operative nTMS language mapping and an intraoperative DES tests from the 27 enrolled patients, the nTMS investigation resulted to be with a sensitivity level at 97%, a specificity level at 15%, a positive predictive value at 34%, and a negative predictive value at 91% (Ille *et al.*, 2015a), which supported an earlier study by Tarapore et al. in 2013 (Tarapore *et al.*, 2013).

In terms of feasibility and reliability, previous studies suggested a good consistency of mapping results between nTMS and DES in investigating the language function, therefore, further offering support for the application of nTMS in language studies when considering its non-invades, which can enhance confidence in establishing the nTMS-based customized surgical plan.

2.4.3 nTMS-based Tractography

In the elaboration of surgical plans in neurosurgery, it is not enough to simply rely on the cortical areas localized by nTMS; an underlying sub-cortical evaluation of the language brain structures is also indispensable. So those language-related areas localized by preoperative nTMS-mapping, which were used as seeds for tractography process in previous studies, called nTMS-based DTI-Fiber tracking (DTI-FT) (Krieg *et al.*, 2014; Ille *et al.*, 2015b; Negwer *et al.*, 2017; Sollmann *et al.*, 2020a). It allowed further investigation in subcortical language-related tracts in order to estimate the risk of functional loss related to surgery. Additionally, this kind of personalized functional analytics is well in line with the concepts and principles highlighted in the current widely recognized precision medicine.

In previous studies, the deterministic algorithm was applied to the nTMS-based tractography, and its applicability and reliability have been also confirmed (Frey *et al.*, 2012; Raffa *et al.*, 2016; Sollmann *et al.*, 2018b). From the comparison with tractography from anatomical atlas-based DTI-FT, it could be concluded in Raffa's study that nTMS-based imaging analysis can generate a better view of cortico-subcortical neural tracts at a higher level of reliability (Raffa *et al.*, 2016). Negwer's study in 2017 further confirmed Raffa's results and suggested the preponderance of nTMS-based DTI-FT in repeatability for clinical practice (Negwer *et al.*, 2017).

Based on this approach, the contribution of different brain tracts in language or their relevance to language errors has been investigated in many previous studies. Ille et al.

indicated that fronto-occipital fascicle was correlated with grades of language performances in patients with gliomas located in left perisylvian areas (Ille *et al.*, 2018). In the review by Cristofori et al., it suggested that nTMS might be a promising method for researching to investigate the function arcuate fasciculus in language performance (Di Cristofori *et al.*, 2021).

In fact, a further question that has to be confronted in previous studies is: "Does the structural foundation of language function rely on one single or several fibers or does it depend on the collaboration between multiple cerebral structures?". It is clear that most of the current hypotheses and theories on the structural organization for certain cerebral functions are more in agreement with the latter one. Then, in future studies, function-related nerve fibers need to be considered as a comprehensive network when investigating the functional distribution in the brain. Although in 2020, we had made an attempt to analyze all neural tracts together obtained from nTMS based DTI-FT (Zhang *et al.*, 2020). However, obviously, such work is insufficient without involving graph theory for the analysis, so that it cannot reflect the distribution and functioning of the structural brain network related to language performance (Zhang *et al.*, 2020).

2.5 Supervised Machine Learning in Medical Study

Computer science is increasingly being introduced in medical research. By merging computer science with clinical data, more advanced analytic methods can be employed to execute complicated multidimensional calculations, allowing a better process of data mining to obtain meaningful information under complex conditions. For complicated and multifaceted issues faced in clinical and research settings, this gives a more thorough solution and more comprehensible presentation of data. Concerning complex and multidimensional challenges encountered in clinical practice and research, this provides a more thorough solution and better comprehensible presentation of data. In the context of such complex 3D data sets, such as brain MRI scans, the application of machine learning to the interpretation of functionally relevant connectome properties in structural brain scans is undeniably especially suitable.

Dolz et al applied the classification scheme based on supervised machine learning models to segmentize the brainstem on MRI scans in a multicenter-based cerebral tumor therapy context and found consistent volume estimation and high spatial

similarity concerning expert delineations (Dolz *et al.*, 2016). Applying parameters with pre-established clinical relevance rather than all data in supervised machine learning provides for a deeper comprehension of these theoretical measures while also avoiding analytical outcomes that cannot be outlined within the existing theoretical framework (Deo, 2015).

However, supervised machine learning has not yet been used to predict neurosurgical SRA. The cross-disciplinary projects that are still ongoing to be investigated might be the explanations behind it. In the current study through the application of parameters and indicators from graph theory to make SRA predictions, supervised machine learning provides us with a new perspective on data mining (Uddin *et al.*, 2019). When a single set of data cannot fulfill the prediction model, combining multiple factors and their relationships to the analysis may offer better indications, which are closer to the real functional structure state. After all, the composition of functions cannot attribute to a single indicator.

2.6 Aim of the Current Study

The aim of this present study was to enroll patients with glioma in language-eloquent regions and to apply the graphic analysis including graphic parameters to analyze the cerebral function-related cortical and subcortical structures and their connections to investigate their preoperative organization. Furthermore, the results of the graphical analysis were used to determine the risk of developing early postoperative SRA preoperatively, and supervised machine learning was applied to perform a comprehensive analysis of all indicators with predictive potentials. Given those grounding perspectives, the current study aims to investigate the following foci/aims:

(1) To investigate connectome properties based on graphic theory in the structural network in the patients developing language deficits with tumor in language eloquent regions after operations.

(2) To use the nTMS language mapping to localize the language-positive and -negative sites in patients with and without SRA for inter-group comparison that was applied to identify their differences.

(3) Based on the whole-brain network and its subnetwork analysis to investigate the network characteristics of nTMS language-positive and -negative sites, respectively.

(4) The comparisons of properties from networks composed of brain regions connecting positive and negative mapping regions respectively.

3. MATERIALS AND METHODS

3.1 Ethics

A thorough explanation of the process and potential risks of the current study by our neurosurgeons and researchers was given to all enrolled subjects. Before being included in the current study, all individuals submitted their informed consent under a clear understanding. This project was carried out in our department. All study protocols and workflow were formulated and conducted in conformity with the Helsinki Declaration and its subsequent revisions. The ethical committee at our Klinikum rechts der Isar der TUM authorized and supervised the study protocol (registration numbers: 222/14, 338/16, 2793/10, 5811/13, 223/14, and 336/17).

3.2 Patients and Study Inclusion

In order to standardize the conditions of the enrolled patients, the inclusion and exclusion criteria were established in advance for the current study.

The inclusion standards were shown as follows:

(1) Only adults were enrolled in this study (Age above 18 years).

(2) No aphasia detected preoperatively.

(3) Their subjects' primary mother tongue must be German.

(4) Their primary diagnosis must be glioma, which should be later confirmed by the consecutive pathological findings.

(5) Glioma should be located within left perisylvian regions and adjacent to the arcuate fasciculus (AF)-related cortical and subcortical areas

(6) The subjects should be without previous cranial surgery or other intracranial invasion operation.

(7) Written informed consent should be officially documented.

The patients were excluded when they were in the following situations:

(1) Patients are with other neurological or psychiatric diseases besides the cerebral

glioma, including Alzheimer's disease, hemorrhagic or ischemic stroke, leukoaraiosis, etc.

(2) General nTMS (e.g., with cochlear implants, pacemakers, etc.) or MRI scanning exclusion criteria (e.g., claustrophobia, etc.).

(3) With impaired comprehension function and/or being incapable to conduct the language task, for example, consciousness disorders, mental retardation, etc.

(4) Impairment of language function caused by glioma or other diseases.

(5) Only receiving biopsy without glioma resection.

From our database of patients who underwent nTMS language mapping between 2016 to 2019, 62 individuals without prior aphasia diagnosed with left-hemispheric perisylvian glioma and receiving tumor resections in our neurosurgery department were considered feasible and enrolled in the current study.

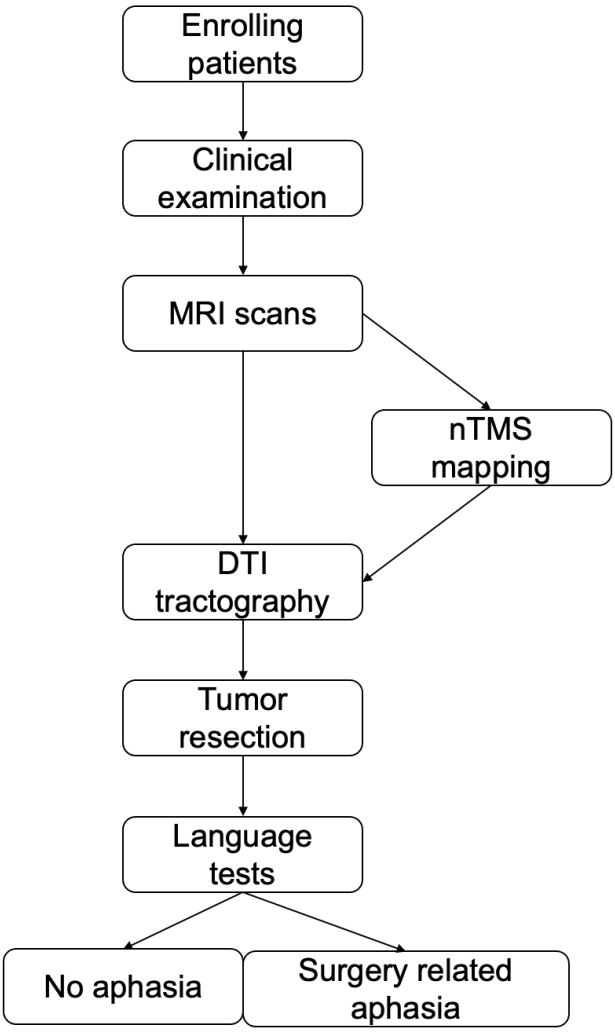

Figure 1

This figure is to present the process of the current study

3.3 Design of the current study

To identify the presence and extent of aphasia, all patients in our center routinely underwent a preoperative clinical examination and speech function assessment. The Aachen Aphasia Test (AAT) was routinely applied to measure the patients' language performance and conducted by our trained neurosurgeons and neuroscientists with this specialized working experience of more than 3 years (Huber *et al.*, 1984; Biniek *et al.*, 1992; Wacker *et al.*, 2002; Sollmann *et al.*, 2015a; Sollmann *et al.*, 2018a). Meanwhile, the handiness side was assessed by our neuroscientist or neurosurgeons according to the Edinburgh Handiness Test (Futai, 1977). Based on these data, we identified patients who did not have preoperative aphasia and enlisted them in the study.

Furthermore, since patients have been with more or less physical and mental weakness because of the brain tumor. Karnofsky's performance status (KPS) was conducted to assess cancer patients' capacity in carring out daily activities through a rating system varying from 0 to 100 (Peus *et al.*, 2013). Only when the patient's KPS scores above 80 can it be assured that the patients will be able to perform the language task properly (Peus *et al.*, 2013).

During their hospitalization, any occurrences of seizures and antiepileptic drug intake will be documented to estimate the risk of new episodes induced by nTMS mapping, although previous studies have shown their associated risk ratios to be very low(Lerner *et al.*, 2019; Stultz *et al.*, 2020). All enrolled patients with low risk ratios were administered routine preoperative MRI scans, followed by nTMS language mapping. Subsequently, seeds produced from nTMS mapping systems were applied to perform deterministic tractography for each individual to identify the subcortical language-related tracts. The MRI scans, language mapping results from nTMS, and tractography results based on nTMS would be integrated to design the scope and process of tumor resecton in 3D space and later imported into the intraoperative navigation system to assist in identifying those critical cerebral structures.

Patients would come back to our clinic for follow-up visit in the third month after surgery and then their language status would be reassessed according to AAT as in the pre-

operative phase, together with the other clinical examinations. As applied in previous studies (Huber *et al.*, 1984; Kelm *et al.*, 2017; Sollmann *et al.*, 2018a), we categorized the aphasic status into four classes according to its severity, as follows:

(1) Grade 0 is for normal language performance.

(2) Grade 1 is for mild deficits. Patients are capable to carry out normal communication with normal verbal comprehension and/or mild manifestion of amnesic aphasia.

(3) Grade 2 represents a moderate language deficit with adequate communication competence. Patients in this category have mild impairments in verbal comprehension and/or conversational speech, which may be interrupted and/or require repetition to proceed.

(4) Grade 3 represents a severe language deficit. In this category, patients present with severe impairments in verbal comprehension and/or conversational speech, manifested as apparent communicative disorders, after it has been clarified that the patient does not have a hearing impairment per se.

Any language deficits would be documented to compare with their preoperative performance to identify the functional alterations. Eventually, 60 patients completed the three-month postoperative follow-up, and they were separated into two groups: the no aphasia group (NA group, 30 patients) and the SRA group (30 patients) based on whether or not they demonstrated postoperative deterioration in speech function. There were two patients who did not come for their follow-up examinations (missing rate: 3.20%).

3.4 Study protocol about magnetic resonance imaging

All MRI scanning examinations were scheduled in accordance with our hospital's routine consultation programs. The same program has been already applied in other published studies (Ille *et al.*, 2015b; Krieg *et al.*, 2016; M. Krieg, 2017).

A 3T-MRI (Achieva, Philips Medical Systems, Netherlands) was equipped for the imaging. Four main sequences were collected for the present study, consisting of a T1-weighted gradient-echo sequence, an enhanced 3D T1-weighted gradient-echo sequence, and a DTI sequence. Their parameters were set up as followings:

(1) T1-weighted gradient-echo sequence. Scanning parameters: TR/TE (9/4 ms) and 1 mm^3 iso-voxel covering the whole head.

(2) Enhanced T1-weighted gradient-echo sequence . Scanning parameters: TR/TE (9/4 ms), 1 mm^3 iso-voxel covering the whole head, scanning while administering contrast agent (Dotagraf 0.5 mmol/mL, Jenapharm, Jena, Germany).

(3) DTI imaging. Scanning parameters: TR/TE (5000/78 ms), Voxel-size (2 × 2 × 2 mm^3), 32 diffusion gradient directions, and b-value (1000s/mm^2).

The preoperative enhanced 3D T1-weighted images were applied to assess the volume of glioma lesions in IntelliSpace Portal (version 9.0; Philips Healthcare, Netherlands, https://www.philips.iq/en/healthcare/product/HC881072/intellispace-portal-advanced-visualization-solution) and ITK-snap (version 3.7; http://www.itksnap.org/pmwiki/pmwiki.php; released from University of Pennsylvania) and recorded for later analysis.

3.5 Language mapping process by nTMS

3.5.1 Registration

The language mapping tests were conducted preoperatively by our technician for each patient using Nexstim eXimia NBS equipment and system (Version 4.3. Nexstim, Helsinki, Finland). He is with nTMS mapping experience more than 5 years.

Individual enhanced T1-weighted images were imported into the Nexstim NBS system for 3D brain reconstruction, where the stimulation targets for language mapping would be predefined based on the template called cortical parcellation system (CPS) (figure 2). Concerning the distorted cerebral structures caused by pathological lesions, such as bleeding or necrosis inside or surrounding the tumor, automatic parcellation could result in inaccuracy in identifying the brain regions. Here, the parcellation is conducted artificially by our skilled neuroscientists together with a neurosurgeon, meanwhile, the stimulating targets were also defined on the dominant hemisphere according to the guidelines and previous publications from our group (Ille *et al.*, 2015a; Ille *et al.*, 2015b; Krieg *et al.*, 2017; Negwer *et al.*, 2017; Sollmann *et al.*, 2018a). According to this parcellation protocol, the hemispherical brain regions are divided into 21 regions with 46 targets for nTMS stimulation. This target setting process were conducted individually

based on their MRI scans hereby to improve the accuracy of targeting process (Krieg *et al.*, 2017).

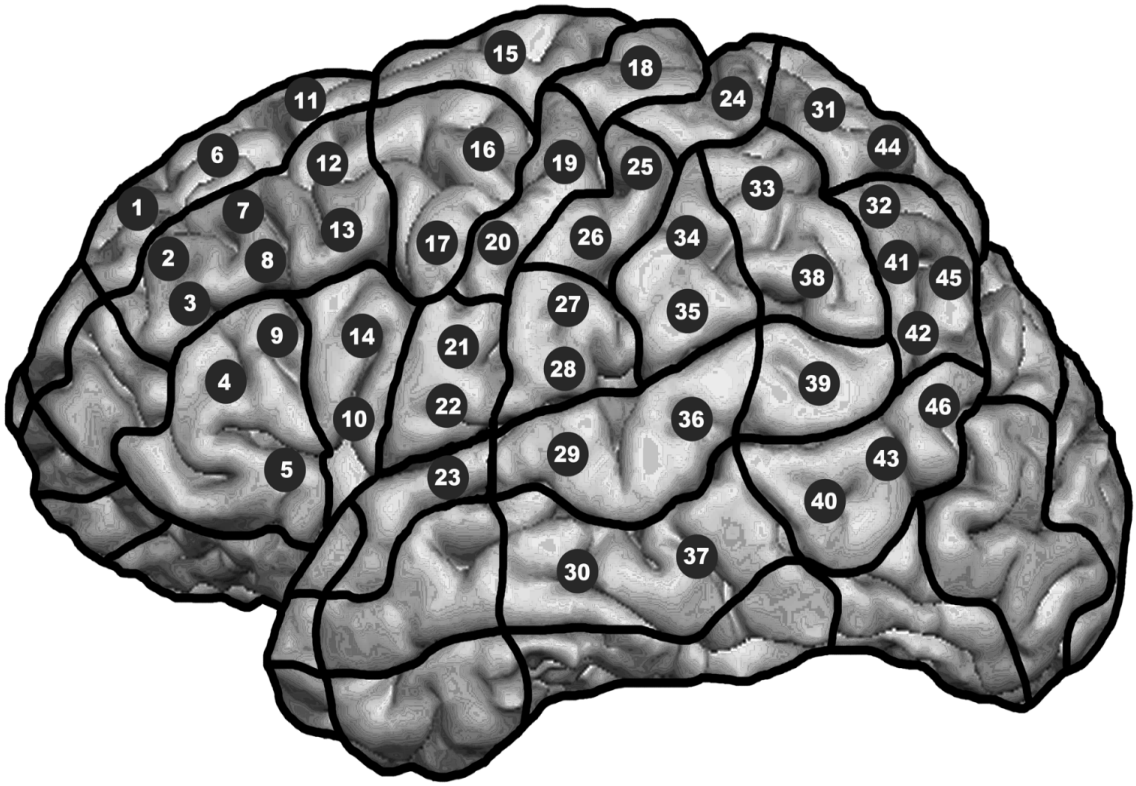

Figure 2. CPS template and cortical 46 targets for nTMS language mapping.

This figure is to presents the template of 46 stimulation targets based on CPS parcellation.

With help of a navigation pen with reflectors, the crux of the helix in both ears together with the nasion were set as landmarks to localize their corresponding positions in the reconstructed 3D-brain so that the individual brain was registered into the mapping system. The patient's forehead is affixed with a star-shaped infrared reflector that can be tracked in real-time by an infrared positioning sensor for the location of the head (Krieg *et al.*, 2017). Subsequent steps were allowed to process in the system only when the registration mismatch level less than 5 mm (Krieg *et al.*, 2017).

Thereafter, the navigation system can automatically match their corresponding coordinates on the reconstructed brain structure in real time, instructing the operator how to adjust the target position of the coil, thus guiding the nTMS stimulus output to the

predefined position from the proper direction and angles with the maximal efficiency.

3.5.2 Rough Mapping to Localize the Hotspot Area

There is a lack of methods to obtain the objective threshold intensity for nTMS stimulation to interfere with language functions (Krieg *et al.*, 2017). It is usually assumed that the action potential of neurons in the cerebral structures is homogeneous, however, the current method for measuring the nTMS intensity thresholds of motor neurons has been well established. According to previous studies and the guideline, TMS mapping in language function adopted the intensity thresholds defined in motor mapping (Ille *et al.*, 2015b; Krieg *et al.*, 2017; Negwer *et al.*, 2017; Ille *et al.*, 2018; Sollmann *et al.*, 2018a).

Electrodes were placed on tendon and belly of muscles, consisting of abductor pollicis brevis (APB), abductor digiti min-imi (ADM), flexor carpi radialis (FCR), and ipsilateral APB on the upper extremity contralateral to the mapping side, to monitor and record motor-evoked potential (MEP) and reaction latency from stimulation output to muscle contraction.

The MEP is considered to be a compound signal originating from a sequence of activated cortico-spinal neurons, and its amplitude generation involved a variety of neural mechanisms, including signal integration and tuning (Krieg *et al.*, 2012; Bestmann and Krakauer, 2015; Krieg *et al.*, 2017). The normal MEP latency for the upper extremity should be within the range from 18 ms to 25 ms. MEP amplitude refers to the absolute peak-to-peak value. A positive site is defined when MEP amplitude value is higher than 50uV (Krieg *et al.*, 2012; Krieg *et al.*, 2017). The coil orientation was related to the direction of its generated electric field and needed to be adjusted to be perpendicular to cerebral gyri in order to maintain the output stimulus reaching the target area at the proper intensity (Krieg *et al.*, 2012; Krieg *et al.*, 2017). The settings of stimulus intensity and stimulus interval were showed as follows:

(1) Stimulus intensity: started at 30% of the maximal coil outputting intensity. When after 5 stimuli no MEP was induced, the intensity should be increased by 5% stepwise.

(2) Stimulus interval: 1.5 s.

The rough mapping was the first step in determining the intensity threshold of stimulus for motor function mapping. Its aim was to identify the most sensitive target on the hand knob region (figure 3), where were supposed to produce the highest MEP amplitude by nTMS with the lowest stimulation intensity (Sollmann *et al.*, 2020b; Wang *et al.*, 2020), called hotspots (Krieg *et al.*, 2012; Krieg *et al.*, 2017).

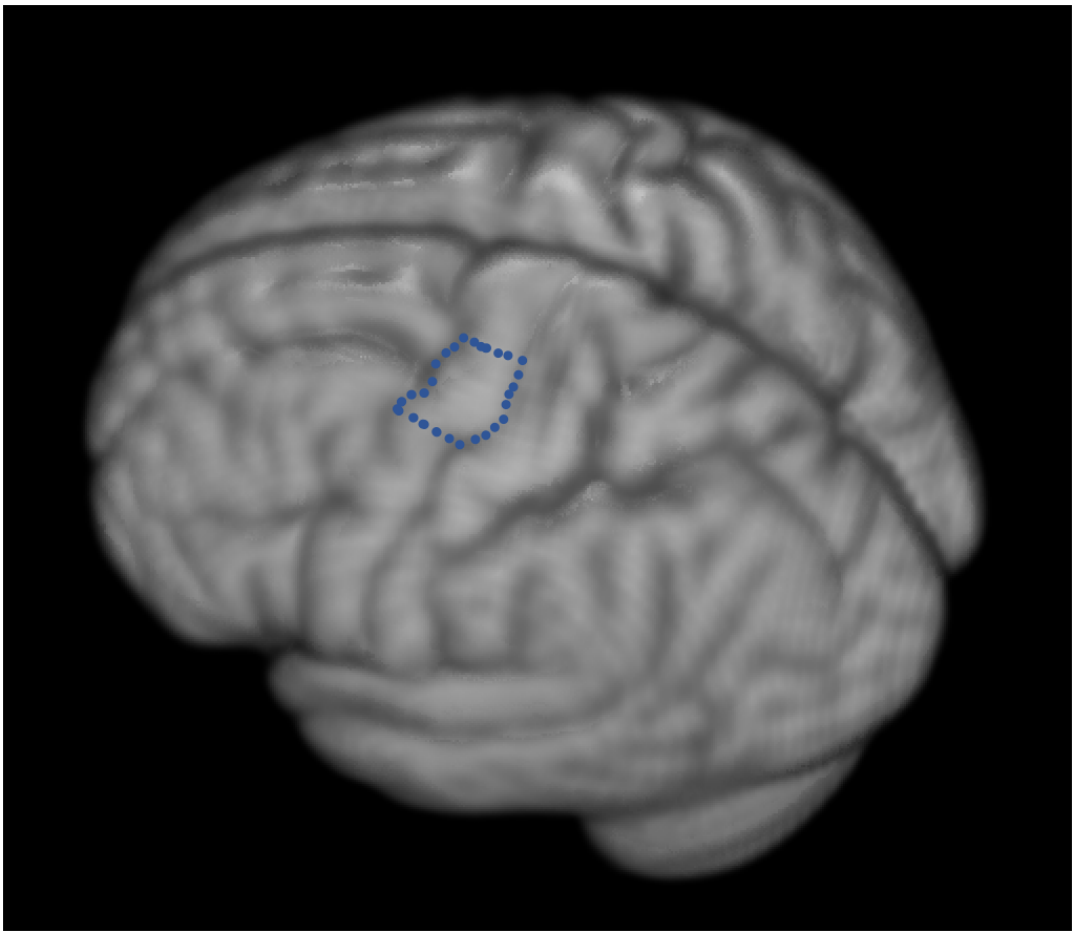

Figure 3. Hand knob

This figure presents the location of the hand knob for nTMS rough mapping (blue dot line).

3.5.3 Identification of the Proper Coil Angulation for Mapping

Targeting the hotspot region, the angulation of the coil was oriented to different angles to identify the angulation most sensitively to induce MEP. At first, at the suggested orientation for the coil by the system, 5 stimuli were sequentially targeted to the hotspot region (figure 4A), thereafter, 5 more stimuli were outputted but using other orientations

at angles other than the suggested one (figure 4B and 4C). Afterward, their corresponding MEPs were recorded and compared to find the highest one and its corresponding angle, which would be used to orient the coil to measure the resting motor threshold (rMT).

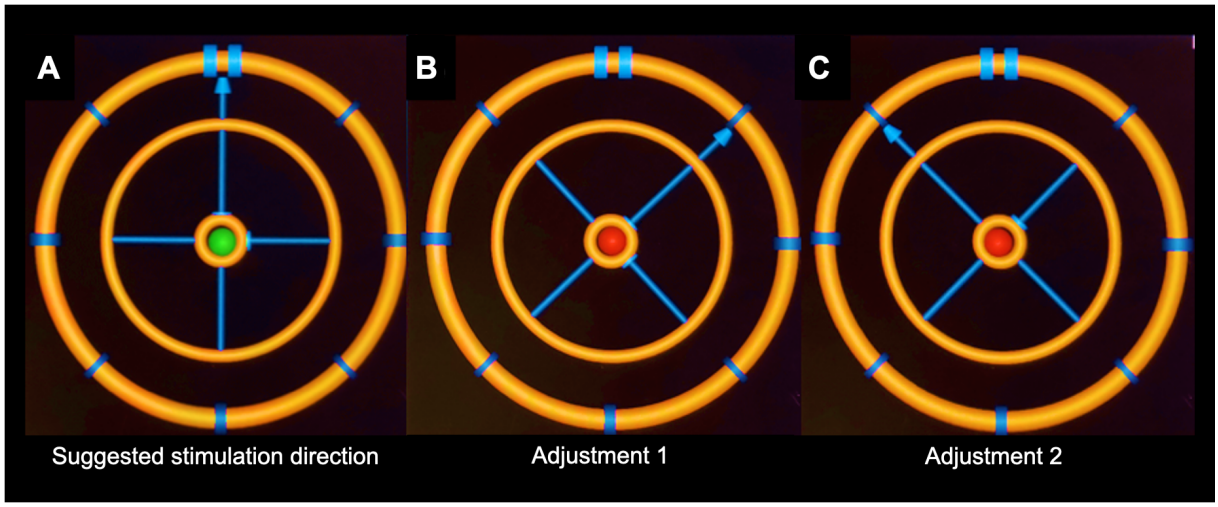

Figure 4. Angulation test.

This figure presents the process of angulation adjustment to identify the optimal direction for later identifying rMT.

3.5.4 Measurement of Resting Motor Threshold

Based on the standard predefined in previous articles, rMT was considered to be the lowest intensity, at which the stimulation was able to induce 5 positive MEPs out of 10 sequential stimuli targeting the same location of hotspot under the same orientation setups (amplitude being more than 50μV and latency between 18~25 ms) (Groppa et al., 2012). From above, the most sensitive hotspot and angulation were acquired and used for measuring the rMT, which was measured for each patient. The nTMS system can meanwhile automatically adjust the output intensity based on the MEP amplitude until the certain intensity that fulfilled the rMT criteria was determined (figure 5).

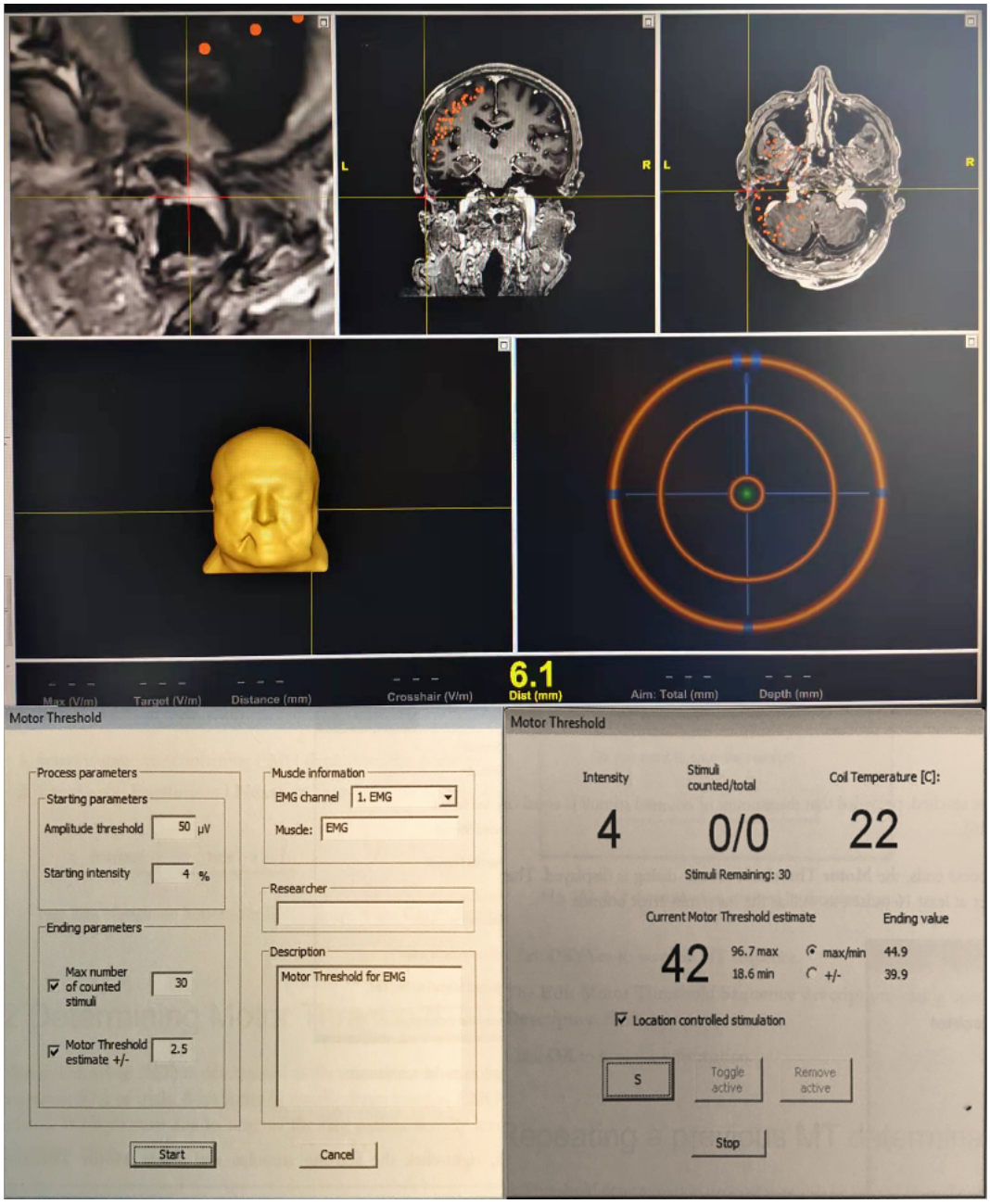

Figure 5. nTMS setup and interface for rMT definition

This figure shows the basic setup in the nTMS system and its interface for rMT measurement.

3.5.5 nTMS Language Mapping

Prior to the examination, it is needed to let the patient be familiar with procedures in the language task and the objects naming task (ONT) examination process aiming to guarantee the quality and reliability of patients' performance during mapping. After their performance fulfills the basic requirements for the mapping, the NBS navigation

software (Version 4.3; Nex-stim, Helsinki, Finland) would orient the nTMS coil to stimulate the predefined 46 targets on their 3D-reconstructed hemisphere when patients conducting the ONT task.

The general protocol for nTMS language mapping is presented below:

Step 1. Device settings

The patient was instructed to seat in a semi-reclining position, and the monitor for the speech task was positioned at about 30-50 cm distance to the eyes. Make sure the patient can clearly see the objects displayed on the screen. All the objects were drawn in black lines with a white background (figure 6). The displaying time was 700 ms with an interval of 2500 ms and adjusted for achieving the patients' best performance. The patients were asked to name the objects shown on the screen in one German word without an article/determiner.

The patient's initial ONT performance was recorded as a baseline in performing the task programs and naming objects on the screen.

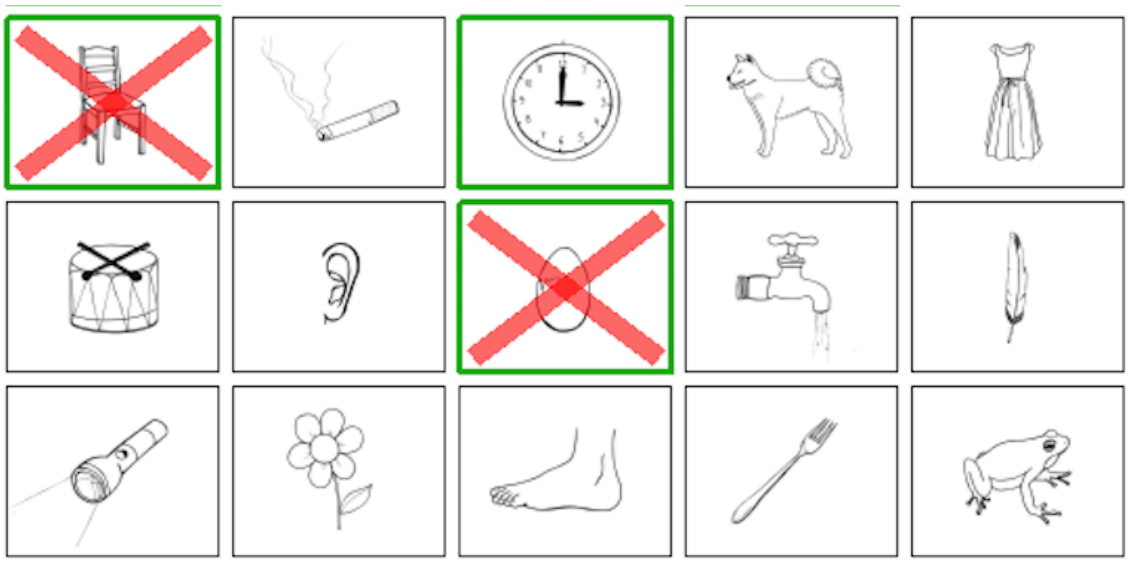

Figure 6. Objects for naming task

This collection of figures shows objects examples presented during named tasks.

In the ONT test, these objects will be displayed on the screen in a sequential manner (Figure 7). Objects that are unfamiliar to the patient or that cause the patient to show hesitation will be excluded, which will be marked with a red cross in the NBS system

and will be excluded in the subsequent steps.

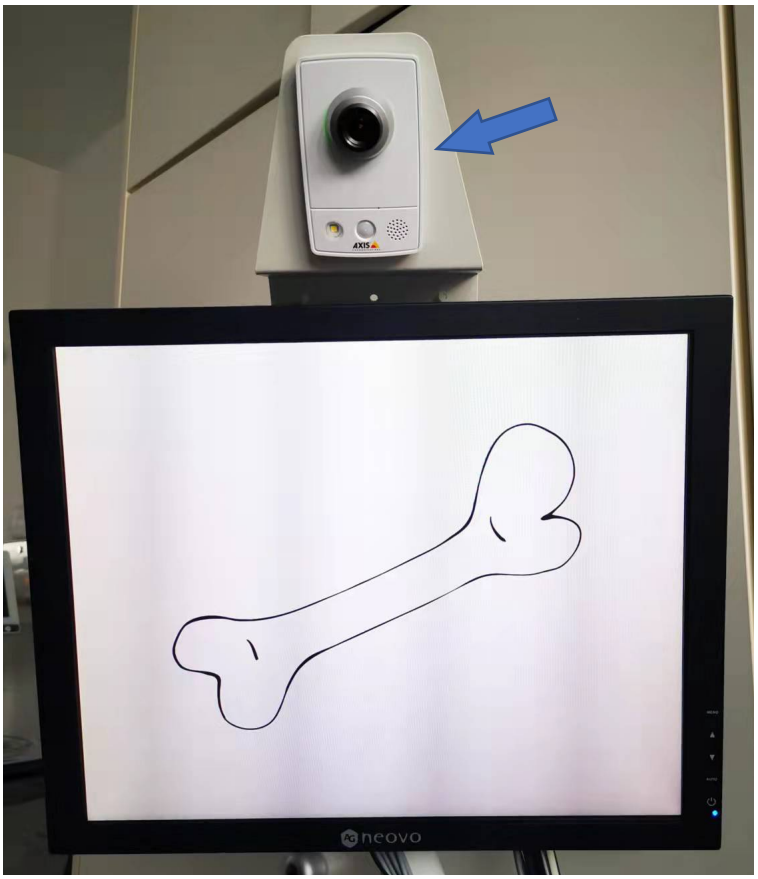

Figure 7. Object presenting and video recorder

The blue arrow in Figure 7 refers to the video recording device that is intended to record the subject's performance in carrying out the object naming task (ONT).

Stimulus-free baseline performance will be recorded for comparisons with the recording of the ONT performance under stimuli.

Step 2. Baseline of ONT

There were two sessions in the baseline test, in which patients were asked to do ONT without stimulation and their performance would be recorded by a high-definition (HD) camera set above the screen (figure 7). The patient's response to the displayed objects was automatically matched and recorded (Krieg *et al.*, 2017). The initial test session was for patients to become acquainted with the objects displayed, after which their unfamiliar or confusing ones would be omitted from the subsequent mapping steps (figure 6).

Depending on their response, if 8 out of 10 displayed objects would be named correctly and/or timely, the display time or interval of objects will be progressively extended by 0.5 seconds each time. Those test adjustments and familiarized figures were applied in the second baseline test to obtain the patient's stable ONT performance (Krieg *et al.*, 2017).

A rest-pause lasting 10 to 15 minutes and water between different task sessions would be prepared if needed by patients to restore strength.

Step 3. ONT test performance under stimulation

Then, patients were instructed to do ONT under repetitive nTMS stimulation, which was also recorded by a high-definition (HD) camera set above the screen (Figure 8). All of the object figures and displaying parameters were identical to those used in the baseline test.

Stimuli were outputted synchronized with the object displaying time to 46 targets that were predefined based on the CPS template, 6 times of stimulation per target, and its parameters were set as follows: stimulus intensity at 100% rMT, 5Hz, and 5 pulses/train (Lioumis *et al.*, 2012; Picht *et al.*, 2013).

Patients' responses were also recorded and automatically matched with the corresponding objects and their performances with the identical object in the baseline test.

In the posthoc analysis, experienced TMS technicians and neurosurgeons compare task performance recordings from the second baseline with task performance recordings from the under-stimulation to identify and categorize naming errors into 6 categories based on the definitions listed below (Sollmann *et al.*, 2013; Ille *et al.*, 2015b; Krieg *et al.*, 2017; Zhang *et al.*, 2020):

No responses: patients were noted to be unable to respond verbally to objects on the screen (Sollmann *et al.*, 2020a).

Performance errors: articulatory failings, particularly form-based mistakes that were spluttered or incorrect (Sollmann *et al.*, 2020a).

Hesitations: naming start was delayed. A considerable lag in patients' verbal response compared to baseline performance should be noted, and patients could simultaneously express hesitation (Sollmann *et al.*, 2020a).

Neologisms: A form-based naming mistake was the use of words that are conceivable but do not exist. This differs from the performance error. The latter stands for the distorted articulatory expression of existing words (Sollmann *et al.*, 2020a).

Phonological paraphasias: unintentional replacement, insertion, deletion, or transposition of a proper word, resulting in phonemic changes (Sollmann *et al.*, 2020a). It was also termed literal aphasia, where words are replaced with non-words that preserve at a minimum of half the number of fragments and/or syllables from the original word.

Semantic paraphasias: this is also referred to as verbal aphasia, substituting the intended word for a semantically related or relevant one (Sollmann *et al.*, 2020a).

After comparing their responses to the same object between the baseline and stimulated tests, the patients' naming errors could be identified and categorized according to the criteria described above. Simultaneously, the TMS system would localize the cerebral areas that corresponded to mistakes in naming, accordingly. Those targets corresponding to the language errors and the targets without language errors induced by nTMS stimulation were registered to the space of enhanced T1 weighted images, then, which were respectively titled as positive (POS) and negative (NEG) mapping files and exported from the Nexstim software in NIFIT format for the consequent analysis (Sollmann *et al.*, 2015b; Zhang *et al.*, 2020).

3.6 MRI Data Processing

3.6.1 Registration and parcellation

All the imaging analyses were conducted at the individual level, all the imaging files were transformed into NIFTI format in software dcm2niix (https://github.com/rordenlab/dcm2niix), consisting of DTI, enhanced T1 weighted images, POS mapping files, and NEG mapping files.

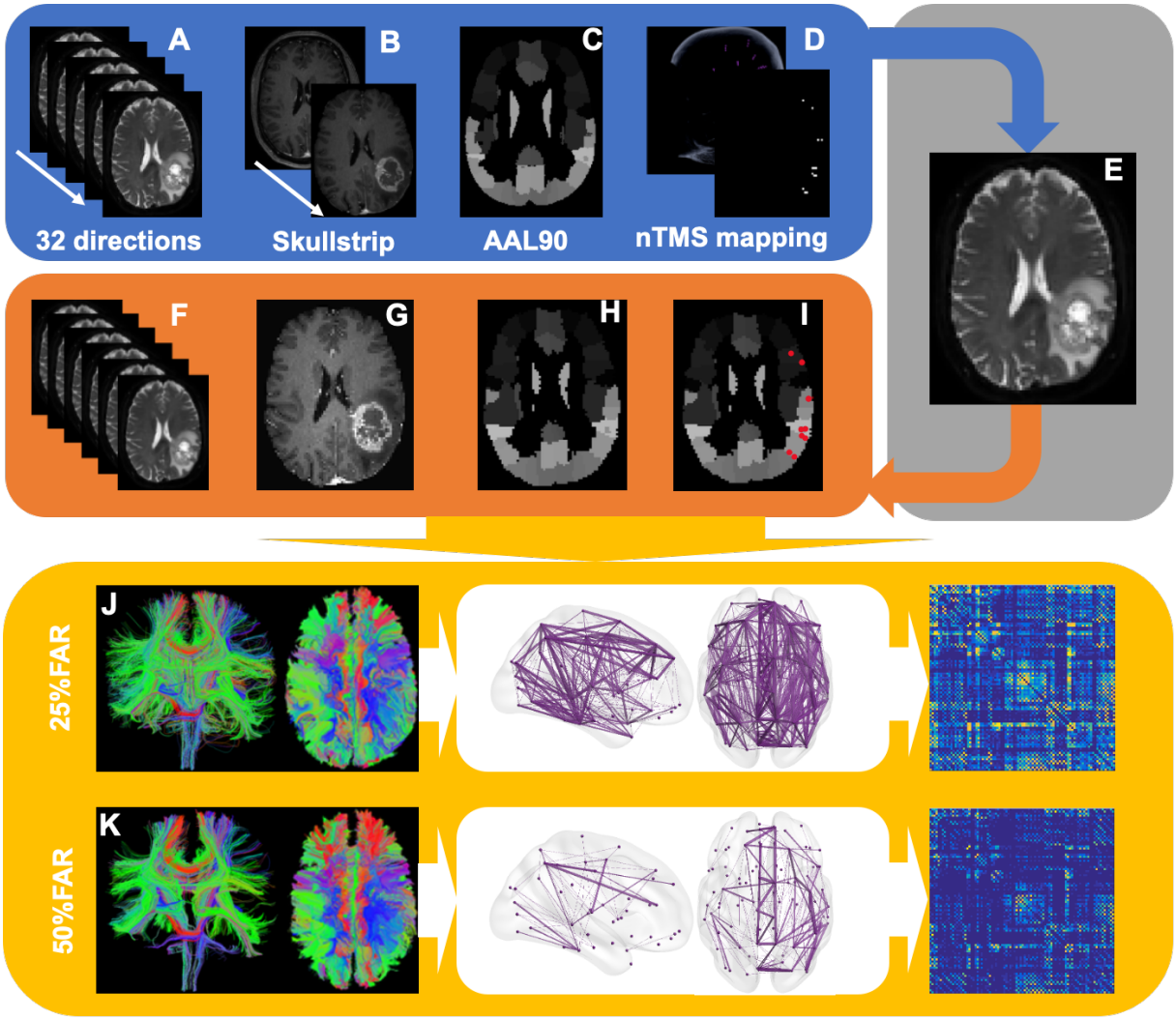

Figure 8. Images processes for the construction of matrices

This figure presents the workflow for processing MRI scans and nTMS mapping results. (A) is for alignment of the 32 direction DTI data. (B) is for the skull stripping process in the T1 weight image with contrast. (C) is the AAL90 parcellation template. (D) is for the results of nTMS mapping data (red points are mapped regions). (E) is B0 image from DTI data. (F) is the (A) registered to (E). (G) is the (B) registered to (E). (H) is the (C) registered to (E). (I) is the (D) registered to (E). (J) and (K) were the results respectively from the fiber tracking when thresholding at 25% and 52% fractional anisotropy ratio, in which the three-dimensional tractography was interpreted into two-dimensional matrices for inter-regional connections.

The processing steps for MRI data were presented as below:

In the first step, the enhanced T1 weighted image was skull-stripped using the HD-

bet toolbox (https://github.com/MIC-DKFZ/HD-BET/).

In the second step, B0 images were extracted from the DTI file for registration using the toolbox in NiBabel (Version 3.2; https://nipy.org/nibabel), which is for the basic structure for DTI scanning.

In the third step, the images from each gradient direction in the DTI files were linearly registered onto the B0 image via Advanced Normalization Tools (ANTs) (http://stnava.github.io/ANTs/) (Avants *et al.*, 2008; Tustison *et al.*, 2013; Tustison *et al.*, 2014) (figure 8 & 9).

In the fourth step, linear registration to the B0-image was conducted for the enhanced T1-weighted images (Isensee *et al.*, 2019), from which the transformation matrices of the conversion process corresponding to each voxel were established (figure 8). Registration was an iterative procedure in which the enhanced T1 weighted images are processed and compared to the B0 image using a similarity measure, including cross-correlation or mutual information (Avants *et al.*, 2011; Isensee *et al.*, 2019) (figure 8).

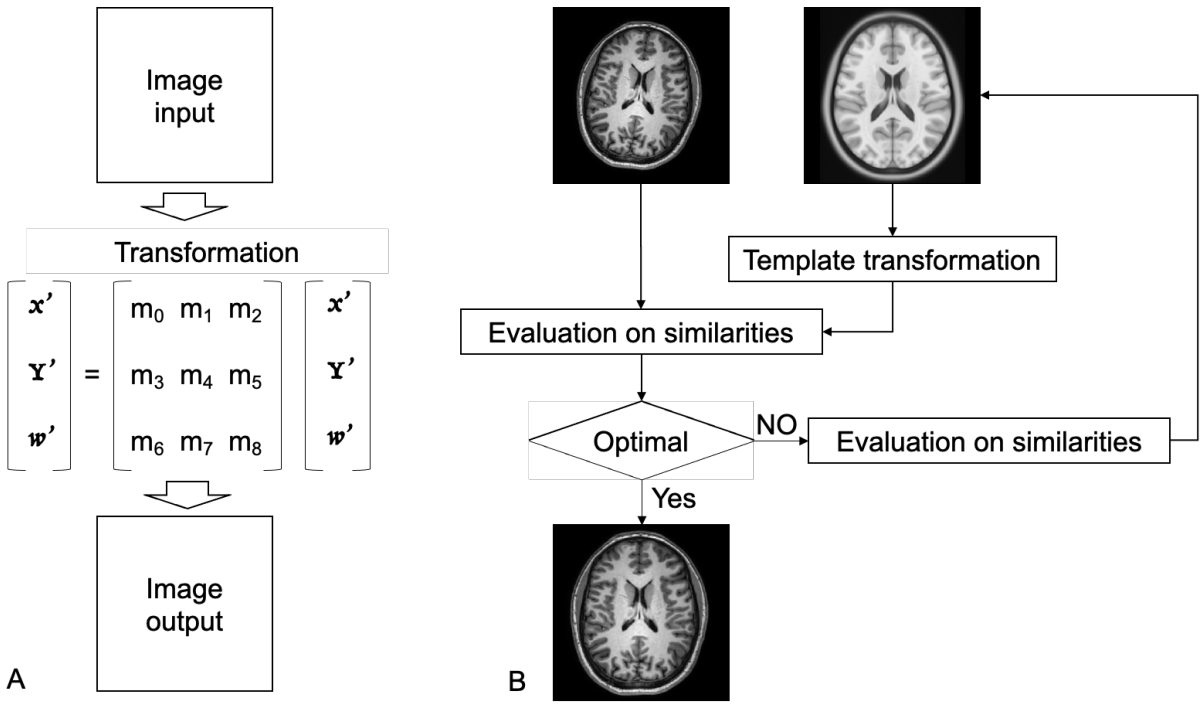

Figure 9

This figure presents the registration process and algorithms used in the ANT toolbox.

In the fifth step, since these POS and NEG files were built based on the same space as enhanced T1 weighted scans, the transformation matrices from Step Fourth can be applied to their registration process to the B0 image (figure 8).

In the last step, the atlas template AAL90 was deformably registered to the B0 image for the structural parcellation (figure 8).

Those registration steps aimed to identify and parcellate the cerebral structures according to the template to the individual level.

This registration workflow enabled the cerebral structures to be individually identified, through which atlas regions corresponding to the mapping points can be respectively identified in POS and NEG images. As a result, the locations in the AAL90 atlas template corresponding to the targets mapped in POS and NEG files can be also identified.

3.6.2 Tractography construction

The tractography for the whole brain was constructed stepwise using Diffusion Imaging In Python (DIPY 1.2.0, https://dipy.org) Python 3.7 (https://www.python.org/). Those processes were presented as below:

(1) Diffusion signal pre-processing

This step consists of data loading, background removal, and gradient table construction for the abstract representation of the acquisition parameters (Avants *et al.*, 2011).

(2) Reconstruction of diffusion distributions in voxels

In DTI files, the diffusion propagator was described by a single 3D Gaussian distribution. Then the constrained spherical deconvolution model using two major constraints on the fitting of the fiber orientation distribution function (fODF) was applied(Tournier *et al.*, 2007), then to identify the maximal values (peaks) of from the model (Tuch, 2004; Avants *et al.*, 2011).

(3) Fiber tractography

A deterministic algorithm is used and seeding based on each voxel in the brain. The seed points were constrained by the volume's dimensions to become the starting sties for the tracking propagation for a streamline, which was based on using Euler's approach suggested by Yeh et al. (Yeh *et al.*, 2010).

Deterministic streamlines were designed to track a predictable trajectory in the imaging datasets by selecting a single major diffusion direction to extend at each voxel, which was limited by the preset threshold on FA, tracking angulation ranges, and tracking lengths. In our current study, tracking angulation rang-es were less than 25 degrees, and fiber length should be more than 30 mm to exclude the U-fibers (Song *et al.*, 2014). During the tracking process, the FAT started at 0.01 and then increased stepwise at 0.01 till minimal fibers were tracked, and the corresponding FAT was at the maximum value (FAT_{max}). All the matrices corresponding to each FAT were transformed into a 90*90 matrix based on the AAL90 parcellation and documented (Zhang *et al.*, 2021a). The maximum FA for every single tract was recorded as fa_{max}, then the FA ratio (FAR) was calculated by the formula:

$$FAR = \frac{fa_{max}}{FAT_{max}} * 100\% \qquad \text{(Zhang } et\ al.\text{, 2021a)}$$

3.7 Graphic Theory Analysis on Structural Connectome

3.7.1 Connectome construction and binarization

For the construction of the connectome, two FARs were implemented as thresholds to choose the matrices, consisting of FAR ≥ 25% and ≥ 50%. Accordingly, those fibers were selected respectively to form connectome matrices together with their corresponding nodes. Seven categories of connectome matrices were formed as below:

(1) M_{whole} was for the whole brain matrix.

Vertices and Edges: both hemispherical regions and their corresponding connections between every two regions.

Size: 90 nodes * 90 nodes.

(2) M_{left} was for the left hemispheric matrix.

Vertices and Edges: left hemispherical regions and their corresponding connections between every two regions.

Size: 45 nodes * 45 nodes.

(3) M_{right} was for the right hemispheric matrix.

Vertices and Edges: right hemispherical regions and their corresponding connections between every two regions.

Size: 45 nodes * 45 nodes.

(4) $M_{pos\text{-}rela}$ was for a matrix consisting of positive mapping regions and their related regions.

Vertices and Edges: positive mapping regions and their related regions, and their corresponding connections between every two regions.

Size: individually defined

(5) $M_{neg\text{-}rela}$ was for a matrix consisting of negative mapping regions and their related regions.

Vertices and Edges: negative mapping regions and their related regions, and their corresponding connections between every two regions.

Size: individually defined

(6) M_{pos} was for a matrix consisting of positive mapping regions.

Vertices and Edges: positive mapping regions and the corresponding connections between every two regions.

Size: individually defined

(7) M_{neg} was for a matrix consisting of negative mapping regions.

Vertices and Edges: negative mapping regions and the corresponding connections between every two regions.

Size: individually defined

Because the sizes of the individual brains and glioma varied, binarizing the fiber number can reduce the interindividual volumic differences. Similarly, tracts between very two regions in all categories of connectome matrices were binarized to “1” when fiber counts were above 3 or to “0” when fiber counts were not above 3.

3.7.2 Graphic analysis

All graphic analyses were conducted through the NetworkX library (https://networkx.org/, https://github.com/networkx/) also in Python 3.7. There are four graphic metrics representing the properties of the connectomes, consisting of:

(1) Average Degree (AD)

AD represented the connection density in a connectome. It is calculated based on the quantity of edges divided by the quantity of nodes (Latora and Marchiori, 2001; Wang *et al.*, 2010).

(2) Average shortest path lengths (AL)

AL stood for the average of the shortest edges in the path between two nodes in the whole network, demonstrating the network's intensity and density (Rutter *et al.*, 2013; Zhang *et al.*, 2021b).

(3) Global Efficiency (EG)

The purpose of EG is to assess the effectiveness of parallel information transmission and integrated processing. The concept of EG, which is the inverse of the average shortest path, is related to that of the average shortest path (Latora and Marchiori, 2001; Wang *et al.*, 2010).

(4) Local Efficiency (EL)

The purpose of EL is to assess the efficacy of communication between a node's neighbors when that node is removed. EL of a certain vertex is the inverse of the averaged shortest path steps or weights of all neighbors connected to that vertex (Latora and Marchiori, 2001; Wang *et al.*, 2010).

The creation of all connectome figures was processed in Matlab (Version: R2016b; Academic License to TUM) using the toolbox of BrainNetViewer (https://www.nitrc.org/projects/bnv/) (Xia *et al.*, 2013).

3.8 Statistical Process

All following statistical analysis were conducted using GraphPad Prism (8.4.3, USA. https://www.graphpad.com).

(1) Demographic characteristics comparisons.

The demographic characteristics of the NA and SRA group, regarding handedness, gender, and histopathological diagnosis, were compared through the Chi-square test. Independent t-testing was applied for the comparison of age and glioma size.

(2) Comparison of mapping results.

Intra- and intergroup comparisons of the mapping regions were performed using Chi-Square or Fisher Exact testing.

(3) Similarities in intra-group mapping regions.

Calculation of the intra-group ratio of language mapping regions.

(4) Inter-group comparisons

It was to investigate the differences in the graphic properties of the seven categories of connectome matrices.

(5) Receiver operating characteristic (ROC) analysis

It was to identify the connectome properties with predicting potentials of developing SRA using the Youden Index based on their sensitivity and precision.

(6) Supervised machine learning to predict SRA.

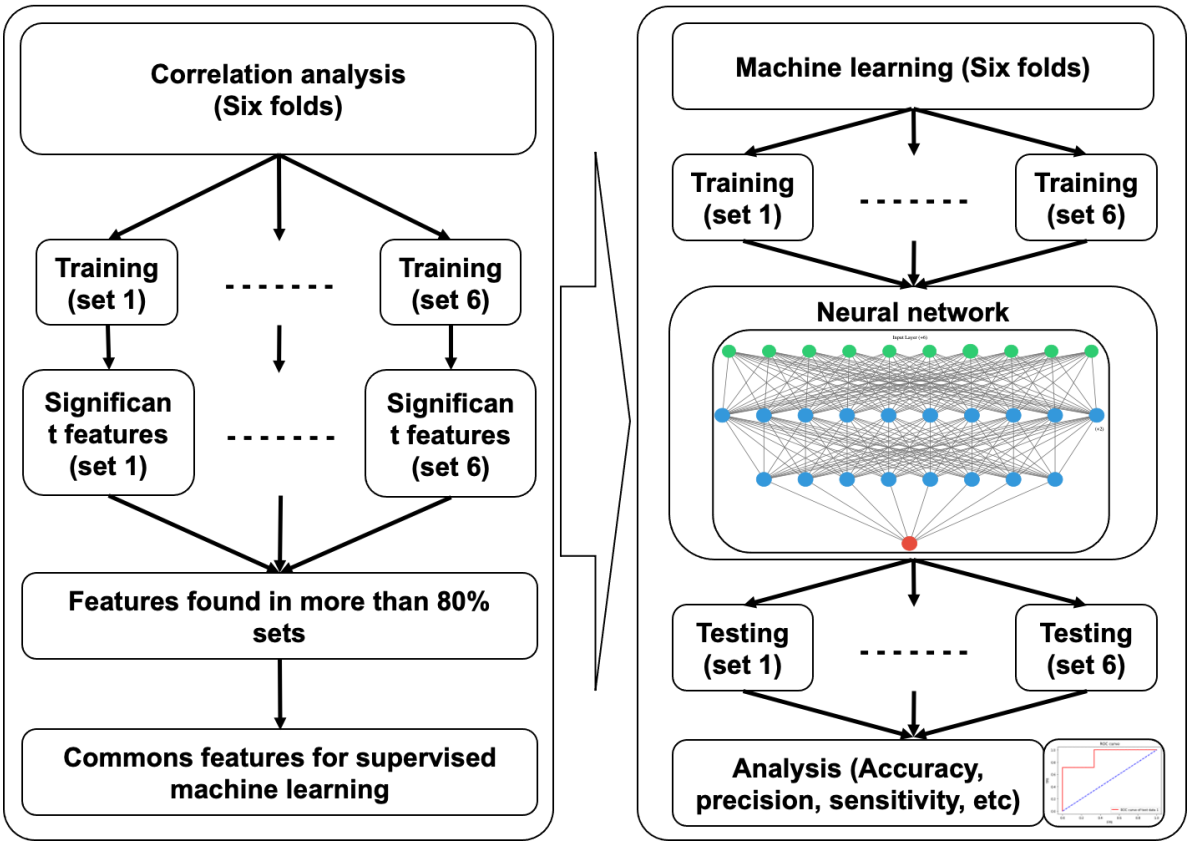

Figure 9. Supervised machine learning process and cross-validation

This figure shows the steps of supervised machine learning and cross-validation

Connectome parameters were used to train a 6-fold cross-validated multi-layer perceptron (with 12->6->1 units and sigmoid output) to predict SRA (Figure 2).

4. RESULTS

4.1 Demographic analysis

No differences in age were detected between the NA patients (59.7 ± 15.1 years) and SRA patients (58.8 ± 15.2 years) (P = 0.327). Glioma sizes in the NA group (2.438 ± 2.630 cm^3) presented no differences to the SRA group (2.829 ± 2.853 cm3) (P = 0.583) (table 1).

The Chi-square test showed no difference for handedness (P = 0.781), gender (P = 0.152), and WHO Grades (P = 0.766) between the NA and SRA group (table 1). The FAT_{max} values of the NA group were at 0.531 ± 0.065 and showed no difference with that of SRA group (0.545 ± 0.053) (P = 0.378) (table 1).

Table 1. Patient Characteristics

Items							Chi-Square	P-value
Handedness	**Left**	NA	4	**Right**	NA	26	0.131	0.718
		SRA	5		SRA	25		
Gender	**Male**	NA	6	**Female**	NA	24	2.052	0.152
		SRA	11		SRA	19		
WHO Grade	**I~II**	NA	8	**III~IV**	NA	22	0.089	0.766
		SRA	7		SRA	23		
Age	**NA:** 59.7±15.1 years			**SRA:** 58.8±15.2 years			**P:**	0.327
							T:	0.988

The Chi-Square testing of patient characteristics, namely handedness, gender, and WHO (World Health Organization) grade of glioma, is presented in this table. It also presented age comparisons between two groups using T-test. No differences were identified between the no aphasia group (NA) and surgery-related aphasia group (SRA).

4.2 Language Mapping Region Analysis

The number of POS areas was considerably smaller than the number of NEG areas in both groups (P = 0.001, figure 10), with no differences in the number of POS and NEG

areas between the NA and SRA groups.

From a detailed analysis on the preoperative mapped areas, no significant differences were detected between NA and SRA patients (Table 2).

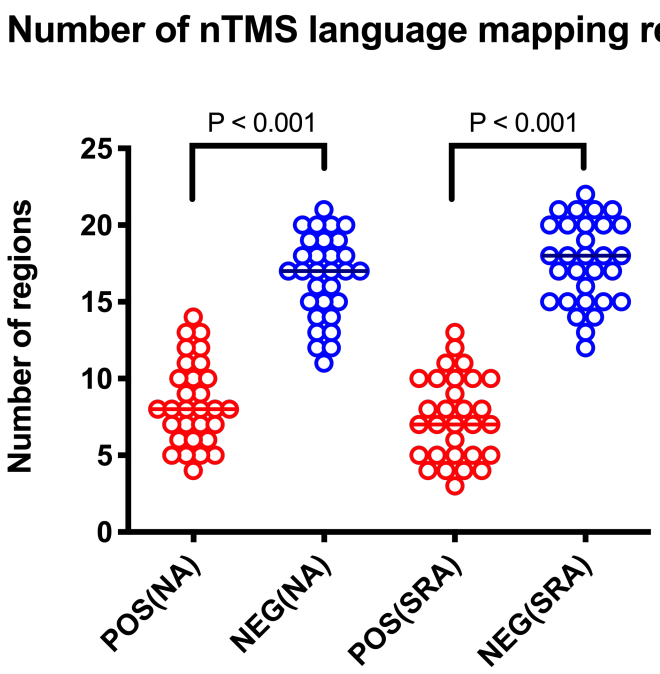

Figure 10. Analysis of counts on mapped areas

This figure shows that the number of positive nTMS mapping areas (POS) is substantially less than the number of negative nTMS mapping regions (NEG) in both groups, when paired t-testing is used. There are no differences in the number of mapping areas between the NA (no aphasia) and SRA (surgery-related aphasia) groups.

Table 2. Comparison of positive and negative mapping regions

Items	Surgery-related aphasia (SRA)		No aphasia (NA)		P-values		
	Counts of POS	Counts of NEG	Counts of POS	Counts of NEG	Chi-Square Test	Corrected Chi-Square Test	Fisher Exact Test
STG	19	11	19	11	\	1.000	\
SMA	5	25	4	26	\	1.000	\
Angular	14	16	13	17	0.795	\	\
PreG	22	8	23	7	0.766	\	\
mSFG	0	30	1	29	\	\	1.000

SOG	0	30	1	29	\	\	1.000
ITG	1	29	2	28	\	1.000	\
MOG	3	27	2	28	\	1.000	\
Rolandic-oper	8	22	9	21	0.774	\	\
PosG	20	10	21	9	0.781	\	\
MTG	24	6	23	7	0.754	\	\
TP	5	25	7	23	0.519	\	\
Heschl	1	29	4	26	\	0.350	\
MFG	25	5	28	2	\	0.421	\
SmG	19	11	16	14	\	0.432	\
IFG-tria	10	20	14	16	0.292	\	\
SPG	11	19	15	15	0.297	\	\
IPG	8	22	12	18	0.273	\	\
SFG	15	15	20	10	0.190	\	\
IFG-oper	13	17	18	12	0.196	\	\

Precentral gyrus (PreG), Supplementary motor area (SMA), medial superior frontal gyrus (mSFG), superior occipital gyrus (SOG), inferior temporal gyrus (ITG), middle occipital gyrus (MOG). Rolandic operculum (Rolandic-Oper), postcentral gyrus (PosG), middle temporal gyrus (MTG), temporal pole (TP), middle frontal gyrus (MFG), supramarginal gyrus (SmG), triangular part of inferior frontal gyrus (IFG-tria), superior parietal gyrus (SPG), inferior parietal gyrus (IPG), superior frontal gyrus (SFG), and parietal opercular part of inferior frontal gyrus (IFG-oper) were showed in the table to show the difference between two groups.

4.3 Graphic analysis on edges

Overall, ADs of different connectome categories in the NA group were higher under both FARs (25% and 50%) than that in the SRA group thresholding respectively: statistically differences between the NA group and the SRA group regarding ADs of the M_{right} (25% FAR: P = 0.044; 50% FAR: P = 0.031), $M_{pos\text{-}rela}$ (25% FAR: P = 0.040; 50% FAR: P = 0.018), and M_{pos} (25% FAR: P = 0.040; 50% FAR: P = 0.046) (figure 13, 14, and 16; table 3). M_{whole} and M_{left} were with higher ADs in the NA group (*P* = 0.023, *P* = 0.037. table 3; figure 11 and 12) only when thresholding at 50% FAR.

Regarding the analysis on the path length, ALs in the M_{right} is significantly smaller in NA patients than that in the SRA patients when FAR threshold was at 25% (P = 0.021. Table 3; figure13).

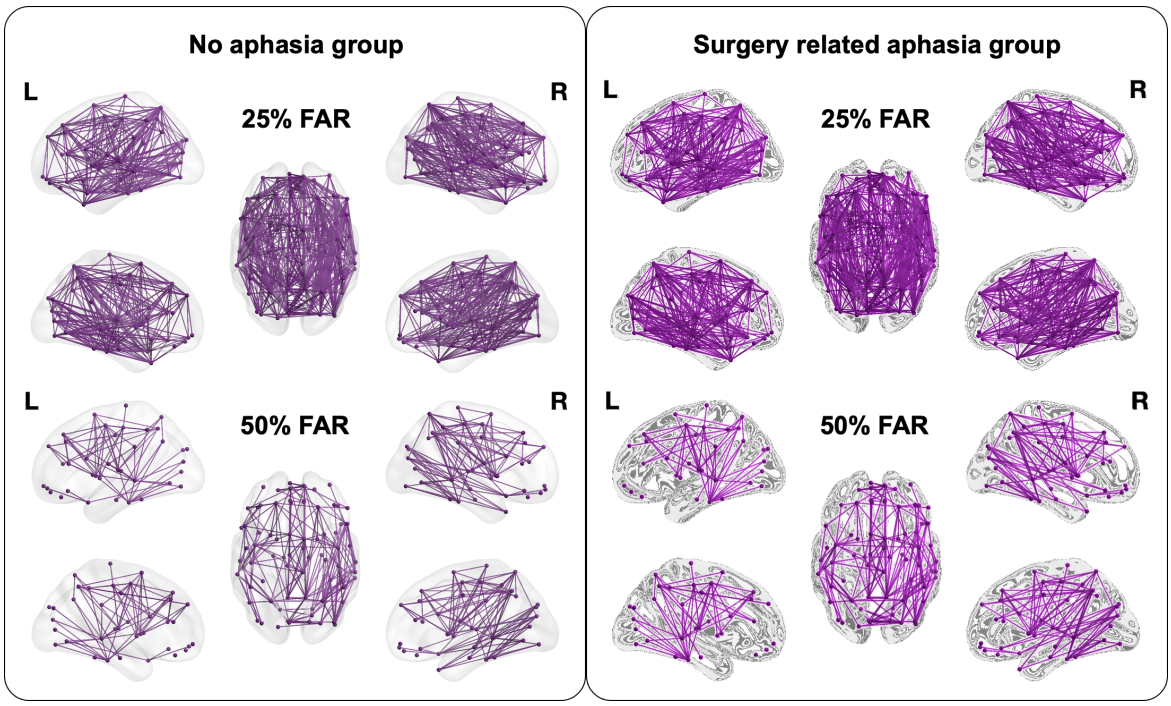

Figure 11. Whole-brain tractography

This figure shows the different tractography of whole-brain network from no aphasia group and surgery induced aphasia group under 25% and 50% fractional anisotropy ratio (FAR), respectively.

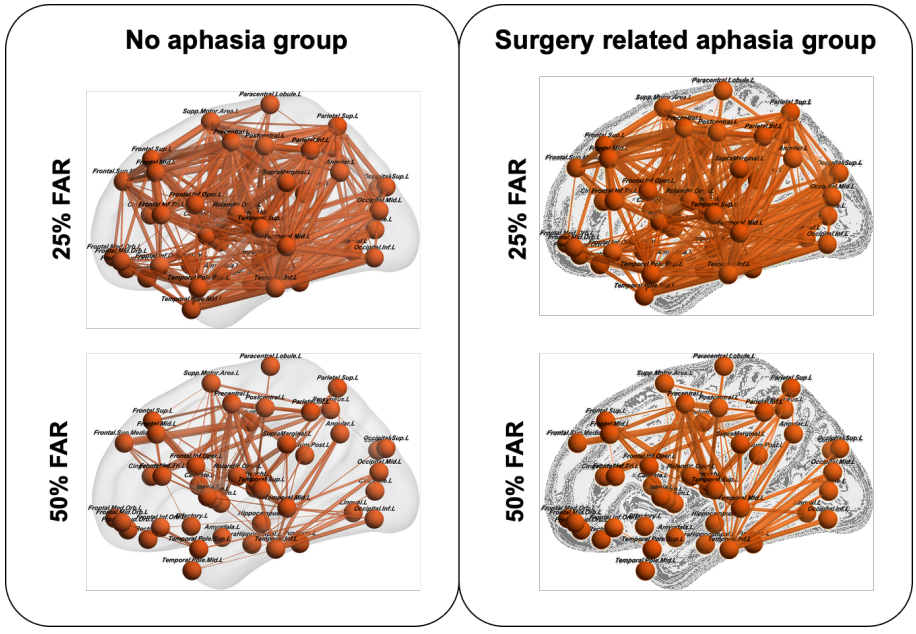

Figure 12. Left hemispheric tractography

This figure shows the different tractography of left hemispheric network from the no aphasia group and surgery induced aphasia group. under 25% and 50% fractional anisotropy ratio (FAR), respevtively.

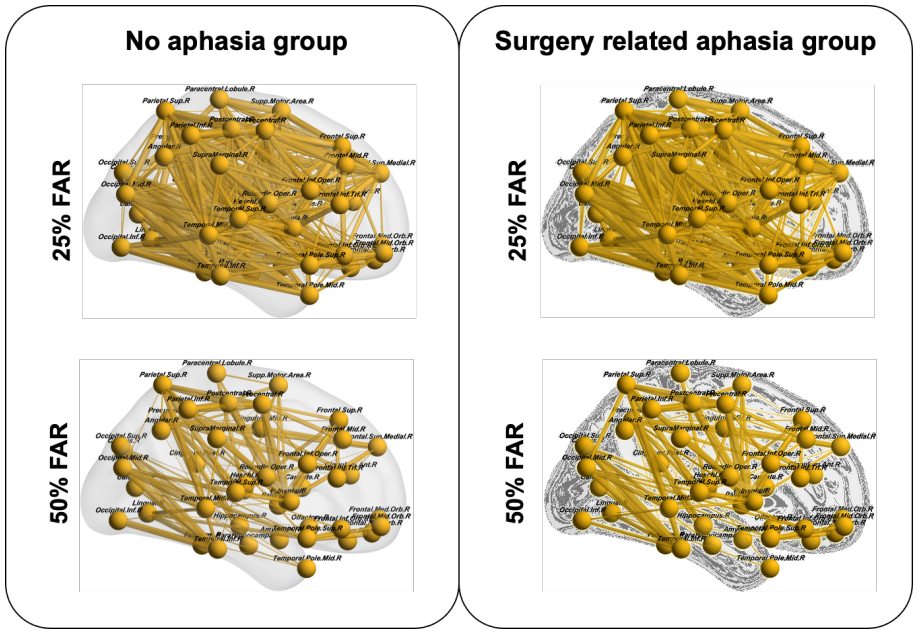

Figure 13. Right hemispheric tractography

This figure shows the different tractography of right hemispheric network from no aphasia group and surgery induced aphasia group under 25% and 50% fractional anisotropy ratio (FAR), respectively.

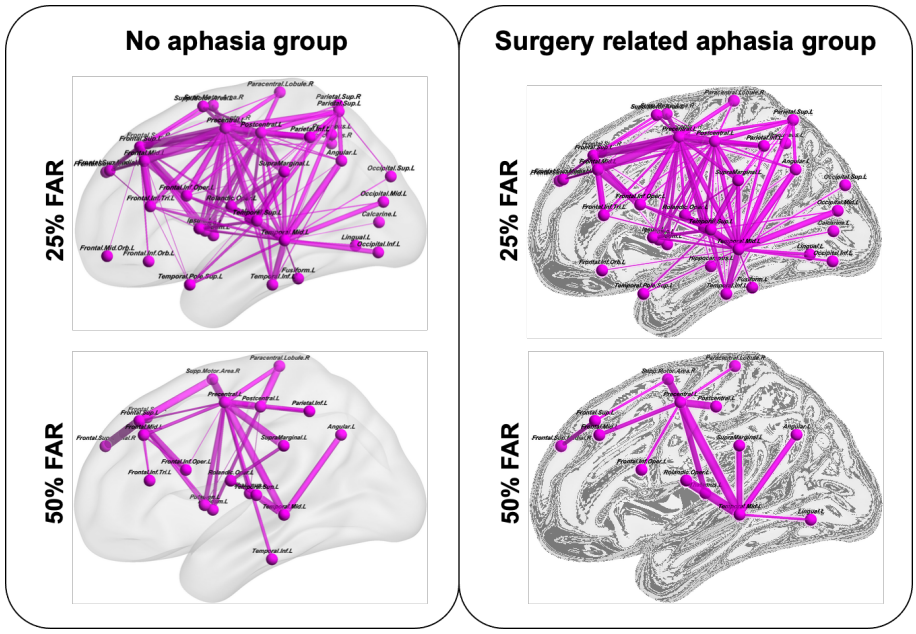

Figure 14. Tractography based on positive nTMS mapping regions and their connected regions

This figure shows the different tractography in the network related to positive nTMS mapping regions and their connected regions from the no aphasia group and surgery induced aphasia group under 25% and 50% fractional anisotropy ratio (FAR), respectively.

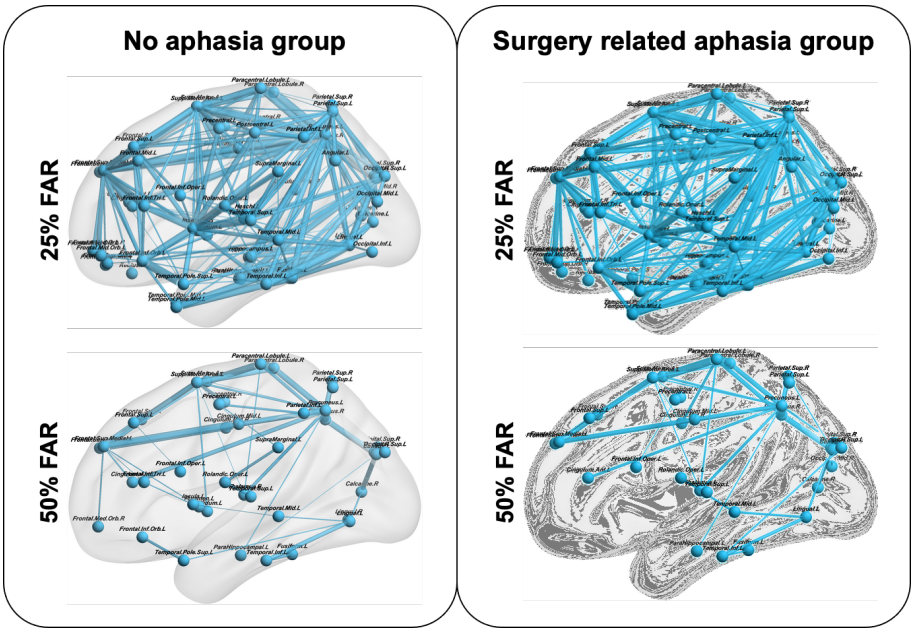

Figure 15. Tractography based on negative nTMS mapping regions and their connected regions

This figure shows the different tractography in the network related to negative nTMS mapping regions and their connected regions from the no aphasia group and surgery induced aphasia group under 25% and 50% fractional anisotropy ratios (FAR), respectively.

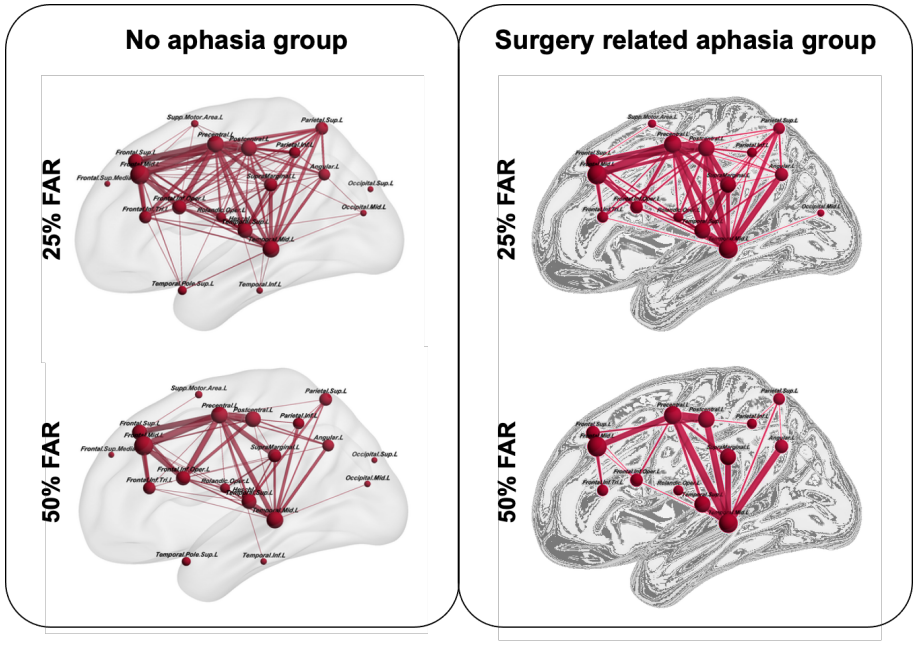

Figure 16. Tractography based on positive nTMS mapping regions

This figure shows the different tractography in the network related to positive nTMS mapping regions from the no aphasia group and surgery induced aphasia group under 25% and 50% fractional anisotropy ratio (FAR), respectively.

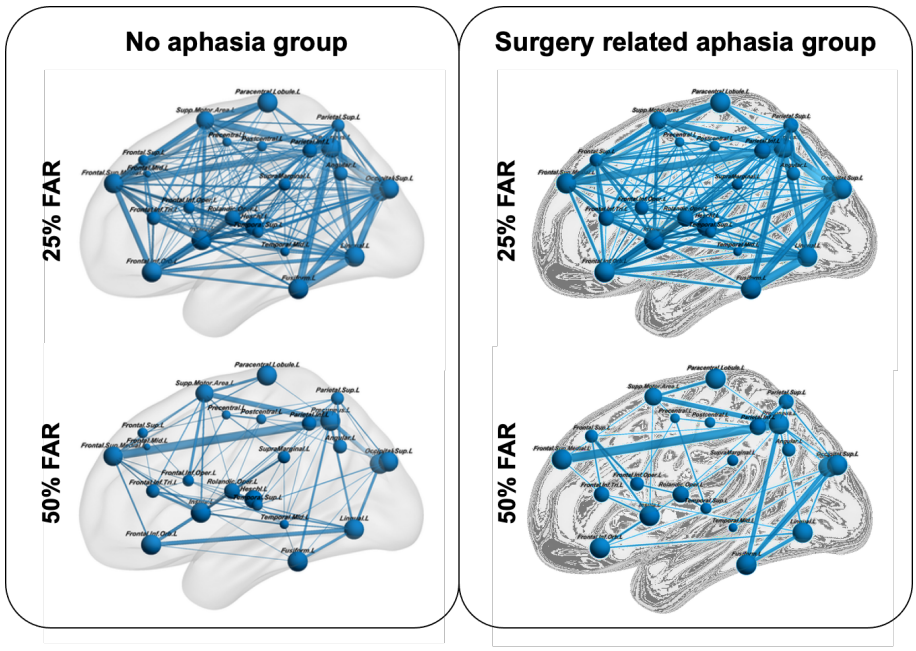

Figure 17. Tractography based on negative nTMS mapping regions

This figure shows the different tractography in the network related to negative nTMS mapping regions from the no aphasia group and surgery induced aphasia group under 25% and 50% fractional anisotropy ratio (FAR), respectively.

Table 3. Analysis on edges

Items		Connectome matrices						
		M_{whole}	M_{left}	M_{right}	$M_{pos\text{-}rela}$	$M_{neg\text{-}rela}$	M_{pos}	M_{neg}
25% FAR								
AD	**NA**	7.635	5.430	5.833	1.896	2.991	2.073	2.392
	SRA	7.073	4.958	5.326	1.624	2.880	1.619	2.205
	p-value	0.054	0.087	**0.044**	**0.040**	0.457	**0.045**	0.344
AL	**NA**	2.079	1.927	1.861	2.235	2.28	1.251	1.901
	SRA	2.121	1.958	1.921	2.254	2.329	1.203	1.953
	p-value	0.091	0.427	**0.021**	0.674	0.264	0.737	0.587
50%FAR								
AD	**NA**	2.863	1.883	2.344	0.733	1.105	0.933	0.766
	SRA	2.358	1.466	1.914	0.552	0.960	0.661	0.583
	p-value	**0.023**	**0.037**	**0.031**	**0.018**	0.182	**0.046**	0.154
AL	**NA**	2.804	2.424	2.547	2.437	2.807	0.942	1.474
	SRA	2.934	2.437	2.411	2.288	2.884	0.617	1.480
	p-value	0.092	0.929	0.214	0.319	0.614	0.090	0.976

This table shows differences of average degree (AD), and the average shortest path (AL) between the no aphasia (NA) group and the surgery-related aphasia (SRA) group thresholding at 25% and 50% fractional anisotropy ratio (FAR). The higher AD of matrices of regions from the right hemisphere (M_{right}), matrices of brain regions with connections to nTMS positive regions ($M_{pos\text{-}rela}$), and of matrices of nTMS positive mapping regions (M_{pos}) was found in the NA patients than that in the SRA patients. ALs identified only in the M_{right} is significantly smaller in NA patients than that in the SRA patients when the FAR threshold is at 25%.

4.4 Graphic analysis of network efficiency

NA group presented higher average connectome efficiencies in EG and EL than those in the SRA group (figure 11 ~ 17; table 3).

The NA group had statistically higher EG and EL from M_{whole} thresholding at both 25%

and 50% FARs when compared to the SRA group (figure 11; table 3). The ELs in M_{left} showed differed significantly between the two groups, while the differences in EG were not significant under 50% FAR (figure 12; table 3). The $M_{pos\text{-}rela}$ and M_{pos} were with higher EGs under both FARs thresholds in the NA group. However, there were no statistical difference in their ELs were detected (figure 14 and 16; table 3). Regarding M_{neg}, its ELs with 50% FAR was significantly lower in the SRA patients (figure 17; table 3). The differences in EGs and ELs between the two groups under both thresholds from $M_{neg\text{-}rela}$ were without statistical significance (figure 15; table 3).

Table 4. Analysis on graphic efficiency

Items		Connectome matrices						
		M_{whole}	**M_{left}**	**M_{right}**	**$M_{pos\text{-}rela}$**	**$M_{neg\text{-}rela}$**	**M_{pos}**	**M_{neg}**
25% FAR								
EG	**NA**	0.537	0.566	0.593	0.300	0.296	0.704	0.595
	SRA	0.520	0.535	0.571	0.271	0.292	0.596	0.548
	p-value	**0.014**	**0.025**	0.078	**0.040**	0.743	**0.050**	0.084
EL	**NA**	2.863	1.883	2.344	0.733	1.105	0.682	0.633
	SRA	2.358	1.466	1.914	0.552	0.960	0.556	0.586
	p-value	**0.037**	**0.005**	0.089	0.122	0.225	0.122	0.247
50% FAR								
EG	**NA**	0.330	0.297	0.371	0.105	0.121	0.437	0.227
	SRA	0.289	0.246	0.314	0.079	0.105	0.323	0.160
	p-value	**0.036**	0.064	**0.017**	**0.026**	0.215	**0.041**	0.078
EL	**NA**	0.367	0.332	0.373	0.133	0.127	0.338	0.174
	SRA	0.306	0.261	0.307	0.098	0.087	0.187	0.086
	p-value	**0.048**	**0.037**	0.070	0.095	0.053	0.095	**0.026**

This table shows differences in global efficiency (EG) and local efficiency (EL) between the no aphasia (NA) group and the surgery-related aphasia (SRA) group under fractional anisotropy ratio (FAR) thresholds at 25% and 50%, respectively. Thresholding at both 25% and 50% FARs, EGs from matrices of whole brain regions (M_{whole}), matrices of left-hemispheric regions (M_{left}), matrices of regions connected to nTMS positive

regions ($M_{pos\text{-}rela}$), matrices of nTMS negative regions (M_{neg}), and matrices of nTMS positive regions (M_{pos}) in the NA group were higher than that in the SRA group. The higher EGs of matrices of the right hemisphere (M_{right}) were only found in the NA group than that in the SRA group under 50% FAR threshold, and under the same threshold, EGs from M_{left} presented no differences between the two groups. ELs from M_{whole} and M_{left} under both 25% and 50% FAR thresholds as well as ELs from M_{neg} thresholding at a FAR of 50% were higher in the NA group as well.

4.5 ROC analysis

The ROC analysis was aiming to identify the connectome properties potentially to predict the SRA developing risks.

EGs from M_{whole} (P = 0.020) and M_{left} (P = 0.027), ELs from M_{left} (P = 0.013), and ALs from M_{right} (P = 0.025) thresholding at 25% FAR were with statistical significances (table 4).

Moreover, thresholding at 50% FAR, more graphic properties were presented to be statistically significant in predicting SRA, consisting of $M_{pos\text{-}rela}$-EG, M_{pos}-EG, M_{whole}-EG, M_{right}-EG, M_{left}-EL, M_{whole}-EL, M_{whole}-AD, M_{left}-AD, M_{right}-AD, and $M_{pos\text{-}rela}$-AD (table 4).

In detail, M_{whole}-EG and $M_{pos\text{-}rela}$-EG were found to be meaningful with both good sensitivity (0.733) and specificity (0.600) compared to other connectome properties (table 4). Although M_{whole}-AD (0.900), M_{left}-AD (0.800), M_{right}-AD (0.900), and $M_{pos\text{-}rela}$-AD (0.867) showed higher sensitivity but accompanied with a lower specificity between 0.433 and 0.567, which were prone to generate false-negative predictions (table 4).

Table 4. ROC analysis of graphic properties

Items	AUC	Cut-off value	Sensitivity	Specificity	Youden Index	p-value
25% FAR						
M_{whole}-EG	0.674	0.533	0.733	0.600	0.333	**0.020**
M_{left}-EG	0.667	0.572	0.70	0.600	0.300	**0.027**
M_{left}-EL	0.687	0.722	0.867	0.500	0.367	**0.013**
M_{right}-AL	0.669	1.866	0.733	0.600	0.333	**0.025**

50% FAR						
$M_{pos\text{-}rela}$-EG	0.650	0.095	0.733	0.600	0.333	**0.046**
M_{pos}-EG	0.652	0.419	0.667	0.600	0.267	**0.044**
M_{whole}-EG	0.663	0.322	0.633	0.700	0.333	**0.030**
M_{right}-EG	0.677	0.370	0.733	0.567	0.300	**0.019**
M_{left}-EL	0.650	0.315	0.700	0.633	0.333	**0.046**
M_{whole}-EL	0.654	0.352	0.700	0.633	0.333	**0.040**
M_{whole}-AD	0.681	2.894	0.900	0.467	0.367	**0.016**
M_{left}-AD	0.647	1.822	0.800	0.567	0.367	**0.049**
M_{right}-AD	0.654	2.522	0.900	0.433	0.333	**0.040**
$M_{pos\text{-}rela}$-AD	0.647	0.784	0.867	0.467	0.333	**0.048**

This table presents the results of the receiver operating characteristic (ROC) analysis, including the area under the curve (AUC), as well as the sensitivity and specificity with statistical significance (P<0.05). Their corresponding sensitivity and specificity regarding average degree (AD), average shortest path (AL), global efficiency (EG), and local efficiency (EL) in predicting surgery-related aphasia (SRA) were calculated thresholding under 25% and 50% fractional anisotropy (FAR) respectively. Seven matrices (M) were analyzed namely matrices of whole-brain (M_{whole}), matrices of left hemispheres (M_{left}), matrices of the right hemisphere (M_{right}), matrices of regions connected to nTMS positive mapping regions ($M_{pos\text{-}rela}$), matrices of nTMS positive mapping regions (M_{pos}), matrices of regions connected to nTMS negative mapping regions ($M_{neg\text{-}rela}$), and matrices of nTMS negative mapping regions (M_{neg}).

4.6 Supervised machine learning analysis

A 6-fold cross-validated multi-layer perceptron was implemented in this machine learning model. The accuracy, precision, sensitivity, and area under the curve (AUC) across six cross-validation folds were presented corresponding to each fold, and their average prediction performance was above 70% (76.7%, 75.2%, 80.3%, and 79.9%; table 5).

Table 5. Cross-validation machine learning model

Fold	Accuracy	Precision	Sensitivity	AUC

1	0.600	0.667	0.667	0.542
2	0.900	0.833	1.000	0.960
3	0.800	0.714	1.000	0.780
4	0.700	0.750	0.600	0.880
5	0.800	0.750	0.750	0.875
6	0.800	0.800	0.800	0.760
Average	0.767	0.752	0.803	0.799

This table presents the machine learning performance of each fold from the cross-validation model and their averages. Their average accuracy, precision, sensitivity, and area under the curve (AUC) are all above 70%.

5. DISCUSSION

The graphic analysis of DTI tractography combining nTMS language mapping from the preoperative phase was adopted in the current study aiming to illustrate the alterations of intracerebral structures in brain tumor patients in terms of three aspects: cortical mapping regions and connections between every two regions and the networks composed by them.

In the study, the complex three-dimensional brain structures are transformed into a two-dimensional graphical analysis, and we establish a new set of investigations and models to provide a new perspective to advance the study of the language-related networks through function-specific connectome properties. The integration of graphic based algorithms and the supervised machine learning model was implemented to determine those patients at risk for postoperative SRA in the preoperative phase.

The current study further emphasizes the importance of the interdisciplinary studies. Firstly, because of the distinctions in specializations, computer science and neurosurgery are both highly specialized professions, and it is difficult to combine their theoretical and research requirements. Secondly, combining computer science with neuroscience research necessitates the foundation of new theoretical frameworks as well as specialized individuals, both of which are now still being sought by many universities. The integration of computing technology and medical practice can greatly advance the optimization of data analysis and improve the applicability of the methodology.

5.1 Methodology consideration

5.1.1 Binarization of the connectome matrices

As well known, there were physiological differences of sizes in brains and cerebral structures between individuals (Llera *et al.*, 2019). Even in the same individual, there were also differences in brain volume at different ages. In MRI scans, those differences could result in the various quantities of cerebral voxels, so the amount and volume of tracts from DTI-FT could differ between individuals. Previous studies have utilized the method of registering individual structural images to the brain atlas template, to eliminate structural differences between individuals. However, this approach involved

multiple imaging processes, for instance, interpolation, and other algorithms that would change the original DTI dataset, which then caused instability in the tractography results based on those registered images when compared with their original images. Especially in glioma patients, this difference could be even greater due to glioma-related structural deformation, edema, hemorrhage, etc. Thus, it is known that since all graphical analysis is based on DTI's data, the manual errors due to multiple image conversion processes would be reduced when the main analysis and calculations are performed based on its original data.

So, in the present study, to avoid extra interferences related to distortion during the graphical data alignment, we used original DTI data to create the tractography without overprocessing except for the necessary data analyzing steps. In addition, to avoid differences in structural volume and fiber quantities between individuals, we applied binarization to the connections in our analysis: one tract with a fiber number above a threshold would be considered an effective connection between these cerebral regions, vice versa, if one track has a number of fibers below this threshold, it was considered as no effective connection. As a result, the differences in the size of the individual brain in MRI were eliminated.

Thus, these processing steps were implemented to control manual errors and to make interindividual comparisons to be available.

5.1.2 Systematic Analysis of Function and Structures Based on Clinical Practice

It is a well-known principle in the biological world that structure determines function (Rout and Sali, 2019), which is substantiated from genetic structures and expressions, protein structures and functions at the microscopic level, to the skeletal muscles and motor functions at the individual level by previous studies (Sarma and Sarma, 1996; Fehrenbach and Herring, 2017; Ramesh, 2019; Rout and Sali, 2019). Without the cerebral structural foundations, the execution and implementation of brain functions were impossible (Honey *et al.*, 2009; Seaquist, 2015; Nahm *et al.*, 2017; Batista-Garcia-Ramo and Fernandez-Verdecia, 2018), which was further highlighted to be related to manifestations in several diseases (Muhlau *et al.*, 2006; Landgrebe *et al.*, 2009; Nahm *et al.*, 2017). For the study on the relationship between brain structures and function, we proposed the concept of anatomy-function-connectome. This enables us to organize, summarize and understand the results of previous studies. With the increasing

number of studies deepening in this area, the anatomy-function-connectome is currently being studied at three levels.

Many previous studies on language function have focused on the engagement and involvement of certain brain regions in language execution and comprehension processes. Those were classified as the first level of anatomy-function-connectome, attempting to clarify cerebral structures related to the language function. From the initial Brodmann area segmentation based on functional manifestations after traumatic brain injury (Krause *et al.*, 1914; Brodmann and Gary, 2006; Strotzer, 2009) to fMRI-based brain segmentation (Ryali *et al.*, 2015; Kauppi *et al.*, 2017) and to Chang's study on DES-based localization of language functions (Chang *et al.*, 2017; Li *et al.*, 2021; Young *et al.*, 2021), they attempted using different methods and techniques to identify one or certain brain regions to which the language function can be attributed. Their results were remarkably advanced and laid the foundation for subsequent studies of brain function distribution.

In recent years, it has been further suggested that brain structures are not independent and single functional units in their functional implementation, but rather collaborate with each other based on their own functional attributes, which has been emphasized by many studies (Horwitz and Poeppel, 2002; van Straaten and Stam, 2013). This belonged to the second level of anatomy-function-connectome, focusing on the analysis combining brain cortical and subcortical structures. In fMRI studies, it has been repeatedly emphasized that brain networks consisting of collaborations and associations between brain regions play an important role in functional execution, and such findings have been supported by EEG, MEG studies (Horwitz and Poeppel, 2002; van Straaten and Stam, 2013). The collaboration with-in and between brain networks concluded in their studies would not exist out of no-where; it is necessary for the subcortical tracts, which serve as the anatomical basis for functions, to provide the intermediates for information interaction and communication between different brain regions (Hanggi *et al.*, 2014). It has also been referred to in studies on cerebral structure, and they mainly focused on subcortical connectivity in language, proposing a number of hypotheses (Honey *et al.*, 2009; Harrison *et al.*, 2021), for instance, the dual-stream hypothesis (Norman, 2002), etc.

Together with previous studies, the present investigation was based on the clinical findings and focused on the relationship between functions and structures at the whole

network level, belonging to the third level of anatomy-function-connectome. The previous mindset in the study was to localize functional regions by fMRI and use DTI to study the subcortical DTI signal changes in the relevant regions (Dijkhuizen *et al.*, 2012; Hakun *et al.*, 2015). Differently from them, the study by Prof. Krieg et al. introduced graphic theory into the analysis and indicated the association between the language impairments because of tumor and the robustness of the structural network in the patient's brain, which provided a new perspective of study (Zhang *et al.*, 2021a).

5.2 Higher efficiencies in connectome from NA patients

The higher network efficiencies were found in connectomes from the whole brain and left hemisphere respectively in the NA group at both global and local levels when thresholding at higher FAR (> 50%) and lower FAR (> 25%). These changes in graphical properties suggest that effects of left-sided gliomas are not limited to one hemisphere but can also potentially induce a brain-wide inhibitory effect on function, which may be latent and not to be detected as clinical manifestation. In this regard, a study by Ries and colleagues using behavioral experiments demonstrated that brain-injured patients counted more on interhemispheric cooperation to select words for object naming tasks, which supports the relevance of reduced connections among regions to the impaired language performance in patients developing SRA after surgery (Ries *et al.*, 2016). Alternatively, from a graph theory view, it was indicated that when a system shows decreased efficiencies, its robustness and stability to resist external disturbances will also be reduced. Considering the surgical injury, the structural network of the NA group may have better adaptability existing preoperatively or better plasticity developed in the postoperative period. However, it cannot be determined because the present study lacked postoperative DTI data to verify this. Furthermore, a study by Schuppert et al. that the global, neural substrates involving in local and global musical information were processed in the melodic and temporal dimensions (Schuppert *et al.*, 2000), which is also a further indication of the collaboration between local and global brain functions.

It was only EG that was statistically higher in the NA group for $M_{pos\text{-}rela}$ and M_{pos}, which were related to the nTMS positive mapping regions, indicating the importance of those regions and the connections between them in the preservation of global functional integrity, which was related to the nTMS positive mapping regions, indicating the

importance of those regions and the connections between them in the preservation of global functional integrity. This is consistent with the results of the AD analysis, which suggested that within the SRA group the connections between the nTMS positive mapping regions were reduced. This may help to understand why language errors were induced when those regions were under inhibitory stimulation. And the answer was that fewer connections between mapping regions for transmitting information in language production and their global compensation became undermined.

Also, this may be used to explain the differences of application between DCS and TMS positive mapping regions found in previous studies. Additionally, their different mechanism in outputting stimulus should be clarified, DES was the direct electrical stimulations inducing complex cellular potential alterations, where the cell membrane is depolarized reaction at the cathode due to current flowing to the outside, and yet it is hyperpolarized reaction at the anode due to current flowing to the inside (Kombos and Suss, 2009), and nTMS is based on magnetic field inducing electrical field to generate cellular hyperpolarization, both of which can be called "transient lesion" without pathological changes (M. Krieg, 2017). So, it is suggestive that using nTMS is primarily for identifying nodes and connections in language-related networks, whereas DES is more focused on detecting certain regions and associated fibers with high-grade importance for language performance (Sollmann *et al.*, 2014).

The organization of language-related cortical regions and subcortical connections can be more comprehensively understood in function-specific connectome analyses, which is of great potential for further investigations on language's structural basis.

5.3 More high-FAR fibers for the NA patients

The average AD was generally higher in the patients with normal language function than the patients developing SRA. $M_{pos\text{-}rela}$ and M_{pos} at the two FARs thresholds were distinct between the two groups, but not for the $M_{neg\text{-}rela}$ and M_{neg}. As mentioned before, $M_{pos\text{-}rela}$ represented the connectome network with nodes consisting of positive mapping regions and their connected regions. At first, with respect to the functional organization, those positively mapped regions served to relay signals in the language-related network, thus connecting other regions and acting as interaction hubs to integrate the language performance signaling. Secondly, with respect to the structural organization,

considering that no difference in tumor size was noted in the two groups, there are two potential explanations for the higher AD in the NA group. Namely, one was that patients in the SRA group initially relied only on the weak connecting tracts to maintain normal functional representation and eventually lost their balance or compensation after surgery, leading to functional deficits, and the other is that patients in the NA group have more compensatory capacity, which possibly induced by glioma, that can mobilize more connections and/or optimize or strengthen existed connections. Although in previous studies it was only shown that the risk of SRA was higher in cases with fewer interhemispheric connections (Sollmann *et al.*, 2017; Negwer *et al.*, 2018), still demonstrated the importance of connection robustness for normal functioning, which had similar findings to the present study.

Compared to the right hemisphere, AD was lower on the left side since the tumors were located in the left hemisphere in both groups. A significant difference in AD was detected between the two groups for connections with FAR > 50%, in addition, statistical tests on FAT_{max} showed no difference. Taken together, this indicated that NA patients have more fibers with high FAR (>50%) than SRA patients. Considering the differences in the functional performance of patients in the postoperative period, it can be inferred that the connections related to language function have higher FA values. Grieve et al. reported that the executive function-FA association was particularly strong and regionally delineated through a voxel-level analysis (Grieve *et al.*, 2007). Moreover, FA values in visual radiation was associated with visual performance at term-equivalent age, and its values from the posterior limb in internal capsule were correlated to cognitive outcomes measured at the first postpartum year (Qiu *et al.*, 2015). Furthermore, in a study on Baduk players, it was shown that after a long time training they had increased FA values in the white matter in frontal, cingulate, and striatal thalamic regions, which involves a functional network of attentional management, work memory, execution modulation and problem-solving procedures (Lee *et al.*, 2010). However, there were some more recent DTI studies reporting that higher FA values can be found in multiple subcortical regions (Mole *et al.*, 2016; Chen *et al.*, 2018) and/or the SN (Lenfeldt *et al.*, 2015). What's more, the current study, focused on the selected subcortical tracts related to the functions and demonstrated that the better prognostic outcome was related to those tracts with higher FA values.

5.4 Potential application for SRA prediction

Predicting SRA during the preoperative period is a difficult challenge in current neurosurgical practice. Plaza et al. reported that in their practice, the tumor infiltration into the inferior frontal gyrus and insular but their resection did not lead to the severe impairments as predicted (Plaza *et al.*, 2009). So, a comprehensive and effective approach is really needed to facilitate clinical treatment decisions to reduce the risk of postoperative aphasia. In the study by Fang et al, it is suggested to predict the postoperative language prognosis in tumor patients based on measuring preoperative MRI scans, consisting of the tumor location and proximity of the tumor toward the superior longitudinal fasciculus/arch fasciculus (Fang *et al.*, 2021). However, it can be found in the implementation that this method was subjective and dependent on the physician's experience, such as defining the border between edema and glioma. The network properties shown in the current study have the potential to serve as important predictors of SRA. However, using one of them alone as a predictor would not yield satisfactory prediction performance. When they are combined to create a machine learning model, it is possible to achieve a sensitivity and accuracy of above 70% in predicting SRA. Although encouraging, this method was still needed to be validated and improved in further studies.

In the present study, it can be found that their mapping localizations were similar between the two groups. In addition, the number of their positive and negative mapping areas respectively was also similar. Considering the absence of clinically detectable aphasia in the NA and SRA groups during preoperative testing, it was reasonable to see their similar cortical mapping results. Remarkably, both groups underwent tumor resection without significant differences in the volume of the glioma. Thus, a subcortical connectome analyzed in combination with cortical function could better reflect changes in brain function, which would be meaningful for further insight into the impact of postoperative outcomes and the development of SRA.

5.5 Limitation

Firstly, from the perspective of data collection, healthy subjects were not included in this study as a control group and the sample size was only 60 cases. By using the cross-validation approach, it is to increase the reliability of the data in the machine

learning operation in this study protocol, it still cannot be ignored that a large sample size for further validation and confirmation is still need.

Secondly, the categorization of language functions in this study was only based on whether they presented aphasia or not and did not provide a detailed analysis of the different levels of language performances.

Third, further follow-up of oncology patients was still essential. Language functions at one month postoperatively were only short-termed. The chances of recovery of language function afterward were still possible though the chances were low though. Moreover, factors such as tumor growth rate and different degrees of infiltration were not included in the analysis, their effect on specific functional connectivity groups needed additional studies to confirm.

Fourth, currently, we have only used DES in a limited number of patients to validate localized areas by nTMS language mapping, so it was not analyzed in the current study. And the limited extent of the bone window made it difficult to validate all language-related positive areas localized by nTMS, let alone the nTMS mapping results on the healthy side. In the future, it is still necessary for multiple research centers to jointly work and expand the sample size to achieve comprehensive analysis.

6. SUMMARY

6.1 English Version

It would be one of the first studies on predicting the risk of postoperative surgery related aphasia (SRA) based on preoperative nTMS language function localization and tractography combined with graph theory analysis.

The primary treatment for intracranial gliomas remains to achieve the maximum surgical resection, i.e., achieve gross tumor resection (GTR). Preoperative functional mapping by navigated transcranial magnetic stimulation (nTMS) together with diffusion tensor imaging (DTI) based on nTMS mapping results is increasingly applied for localization of cortical and subcortical speech eloquent areas. The goal is to enable better surgical risk management. If the risk of language impairments due to surgery can be predicted preoperatively, this could better protect the patient's quality of life.

Previous studies have analyzed the risk of surgery by assessing the tumor lesions in certain brain tracts or in certain brain regions and/or the distance between the tumor and language-related brain structures. Differently from them, the present study focused on a systematic analysis of functionally related structures in the brain, investigating their connections and connectome properties, such as degree and graphic efficiency, and accordingly to evaluate the risk of SRA occurrence.

In this study, 60 patients with left hemisphere perisylvian glioma with normal language function were enrolled, 30 of whom had normal language function after surgery and 30 of whom developed SRA. The function-specific connectome network properties in the brain at different fractional anisotropy ratio (FAR) thresholds were investigated to analyze the preoperative alterations in the SRA group compared with no-aphasia patients, and they were further combined with the application of supervised machine learning algorithms for training and cross-validation to analyze the SRA prediction model. The results showed that preoperative linkage group analysis helped to predict the development of SRA at an accuracy and sensitivity above 70%.

The current study provides a new perspective on combining nTMS and function-specific connectome in machine learning model analysis, which is a systematic investigation of language functions and anatomical structures.

The graph-theoretic analysis of complex brain functions and structures through connectome algorithms can advance our understanding of the relationship between complex networks and functional implementation.

6.2 Deutsch Version

Es könnte eine der ersten Studien sein, die das Risiko einer postoperativen operationsbedingten Aphasie (SRA) auf der Grundlage der präoperativen nTMS-Sprachfunktionslokalisierung und der Traktographie der Fasern in Kombination mit einer graphentheoretischen Analyse vorhersagt.

Die primäre Behandlung für intrakranielle Gliome besteht nach wie vor darin, eine maximale chirurgische Resektion, beispielsweise eine Bruttototalresektion (BTR), zu erreichen. Die präoperative funktionelle Kartierung mittels navigierter transkranieller Magnetstimulation (nTMS) in Kombination mit Diffusions-Tensor-Imaging (DTI) wird zunehmend zur Lokalisierung kortikaler und subkortikaler sprachlich eloquenter Areale eingesetzt. Das Ziel ist, ein besseres chirurgisches Risikomanagement zu ermöglichen. Wenn das Risiko von Sprachstörungen aufgrund einer Operation präoperativ vorhergesagt werden kann, könnte dies die Lebensqualität der Patienten besser bewahren. Frühere Studien haben das Operationsrisiko anhand der Tumorläsionen in ausgewählten Hirnbahnen oder Hirnregionen und/oder des Abstands zwischen Tumor und sprachbezogenen Hirnstrukturen analysiert. Im Unterschied zu diesen Studien konzentrierte sich die vorliegende Studie auf eine systematische Analyse funktionsbezogener Strukturen im Gehirn und untersuchte die Verbindungen und Konnektom-Eigenschaften wie Grad und grafische Effizienz, und dementsprechend das Risiko von SRA zu bewerten.

In dieser Studie wurden 60 Patienten mit einem linkshemisphärischen perisylvischen Gliom und normaler Sprachfunktion eingeschlossen, von denen 30 nach der Operation eine normale Sprachfunktion hatten und 30 eine SRA zeigten. Die funktionsspezifischen Eigenschaften des Konnektom-Netzwerks im Gehirn bei verschiedenen Schwellenwerten des fraktionellen Anisotropieverhältnisses (FAR) wurden untersucht, um die präoperativen Veränderungen in der SRA-Gruppe im Vergleich zu Patienten ohne Aphasie zu analysieren, und sie wurden mit der Anwendung von überwachten Machine-Learning-Algorithmen für Training und Cross-Validierung kombiniert, um das SRA-Vorhersagemodell zu entwickeln. die Entstehung einer SRA mit einer Genauigkeit von 73,3 % und einer Sensitivität von 78,3 % vorherzusagen.

Die aktuelle Studie präsentiert eine neue Perspektive der Kombination von nTMS und funktionsspezifischem Konnektom in der maschinellen Lernmodellanalyse, die eine

systematische Untersuchung von Sprachfunktionen und anatomischen Strukturen darstellt.

Die graphentheoretische Analyse komplexer Hirnfunktionen und -strukturen mit Hilfe von Konnektom-Algorithmen kann unser Verständnis für die Beziehung zwischen komplexen Netzwerken und funktioneller Implementierung vorantreiben.

7. REFERENCES

Ardila A, Bernal B, Rosselli M. How Localized are Language Brain Areas? A Review of Brodmann Areas Involvement in Oral Language. Arch Clin Neuropsychol 2016; 31(1): 112-22.

Arefin TM, Lee CH, White JD, Zhang J, Kaffman A. Macroscopic Structural and Connectome Mapping of the Mouse Brain Using Diffusion Magnetic Resonance Imaging. Bio Protoc 2021; 11(22): e4221.

Avants BB, Epstein CL, Grossman M, Gee JC. Symmetric diffeomorphic image registration with cross-correlation: evaluating automated labeling of elderly and neurodegenerative brain. Med Image Anal 2008; 12(1): 26-41.

Avants BB, Tustison NJ, Song G, Cook PA, Klein A, Gee JC. A reproducible evaluation of ANTs similarity metric performance in brain image registration. Neuroimage 2011; 54(3): 2033-44.

Batista-Garcia-Ramo K, Fernandez-Verdecia CI. What We Know About the Brain Structure-Function Relationship. Behav Sci (Basel) 2018; 8(4).

Bestmann S, Krakauer JW. The uses and interpretations of the motor-evoked potential for understanding behaviour. Exp Brain Res 2015; 233(3): 679-89.

Betzel RF, Byrge L, He Y, Goni J, Zuo XN, Sporns O. Changes in structural and functional connectivity among resting-state networks across the human lifespan. Neuroimage 2014; 102 Pt 2: 345-57.

Biniek R, Huber W, Glindemann R, Willmes K, Klumm H. [The Aachen Aphasia Bedside Test--criteria for validity of psychologic tests]. Nervenarzt 1992; 63(8): 473-9.

Borchers S, Himmelbach M, Logothetis N, Karnath HO. Direct electrical stimulation of human cortex - the gold standard for mapping brain functions? Nat Rev Neurosci 2011; 13(1): 63-70.

Brodmann K, Gary LJ. Brodmann's localisation in the cerebral cortex : the principles of comparative localisation in the cerebral cortex based on cytoarchitectonics. New York, NY: Springer; 2006.

Bullmore E, Sporns O. Complex brain networks: graph theoretical analysis of structural and functional systems. Nat Rev Neurosci 2009; 10(3): 186-98.

Chang EF, Breshears JD, Raygor KP, Lau D, Molinaro AM, Berger MS. Stereotactic probability and variability of speech arrest and anomia sites during stimulation mapping of the language dominant hemisphere. J Neurosurg 2017; 126(1): 114-21.

Chen HJ, Gao YQ, Che CH, Lin H, Ruan XL. Diffusion Tensor Imaging With Tract-Based Spatial Statistics Reveals White Matter Abnormalities in Patients With Vascular Cognitive Impairment. Front Neuroanat 2018; 12: 53.

Cohen JR, D'Esposito M. The Segregation and Integration of Distinct Brain Networks and Their Relationship to Cognition. J Neurosci 2016; 36(48): 12083-94.

Deo RC. Machine Learning in Medicine. Circulation 2015; 132(20): 1920-30.

Di Cristofori A, Basso G, de Laurentis C, Mauri I, Sirtori MA, Ferrarese C*, et al.* Perspectives on (A)symmetry of Arcuate Fasciculus. A Short Review About Anatomy, Tractography and TMS for Arcuate Fasciculus Reconstruction in Planning Surgery for Gliomas in Language Areas. Front Neurol 2021; 12: 639822.

Dijkhuizen RM, van der Marel K, Otte WM, Hoff EI, van der Zijden JP, van der Toorn A*, et al.* Functional MRI and diffusion tensor imaging of brain reorganization after experimental stroke. Transl Stroke Res 2012; 3(1): 36-43.

Dolz J, Laprie A, Ken S, Leroy HA, Reyns N, Massoptier L*, et al.* Supervised machine learning-based classification scheme to segment the brainstem on MRI in multicenter brain tumor treatment context. Int J Comput Assist Radiol Surg 2016; 11(1): 43-51.

Fang S, Liang Y, Li L, Wang L, Fan X, Wang Y*, et al.* Tumor location-based classification of surgery-related language impairments in patients with glioma. J Neurooncol 2021; 155(2): 143-52.

Fehrenbach MJ, Herring SW. Illustrated anatomy of the head and neck. 5th edition. ed. St. Louis, Missouri: Elsevier; 2017.

Frey D, Strack V, Wiener E, Jussen D, Vajkoczy P, Picht T. A new approach for corticospinal tract reconstruction based on navigated transcranial stimulation and standardized fractional anisotropy values. Neuroimage 2012; 62(3): 1600-9.
Futai M. Reconstitution of ATPase activity from the isolated alpha, beta, and gamma subunits of the coupling factor, F1, of Escherichia coli. Biochem Biophys Res Commun 1977; 79(4): 1231-7.
Gargouri F, Messe A, Perlbarg V, Valabregue R, McColgan P, Yahia-Cherif L*, et al.* Longitudinal changes in functional connectivity of cortico-basal ganglia networks in manifests and premanifest huntington's disease. Hum Brain Mapp 2016; 37(11): 4112-28.
Gollo LL, Breakspear M. The frustrated brain: from dynamics on motifs to communities and networks. Philos Trans R Soc Lond B Biol Sci 2014; 369(1653).
Grieve SM, Williams LM, Paul RH, Clark CR, Gordon E. Cognitive aging, executive function, and fractional anisotropy: a diffusion tensor MR imaging study. AJNR Am J Neuroradiol 2007; 28(2): 226-35.
Groppa S, Oliviero A, Eisen A, Quartarone A, Cohen LG, Mall V*, et al.* A practical guide to diagnostic transcranial magnetic stimulation: report of an IFCN committee. Clin Neurophysiol 2012; 123(5): 858-82.
Hakun JG, Zhu Z, Brown CA, Johnson NF, Gold BT. Longitudinal alterations to brain function, structure, and cognitive performance in healthy older adults: A fMRI-DTI study. Neuropsychologia 2015; 71: 225-35.
Hanggi J, Fovenyi L, Liem F, Meyer M, Jancke L. The hypothesis of neuronal interconnectivity as a function of brain size-a general organization principle of the human connectome. Front Hum Neurosci 2014; 8: 915.
Harrison OK, Guell X, Klein-Flugge MC, Barry RL. Structural and resting state functional connectivity beyond the cortex. Neuroimage 2021; 240: 118379.
Henderson F, Abdullah KG, Verma R, Brem S. Tractography and the connectome in neurosurgical treatment of gliomas: the premise, the progress, and the potential. Neurosurg Focus 2020; 48(2): E6.
Honey CJ, Sporns O, Cammoun L, Gigandet X, Thiran JP, Meuli R*, et al.* Predicting human resting-state functional connectivity from structural connectivity. Proc Natl Acad Sci U S A 2009; 106(6): 2035-40.
Horwitz B, Poeppel D. How can EEG/MEG and fMRI/PET data be combined? Hum Brain Mapp 2002; 17(1): 1-3.
Huber W, Poeck K, Willmes K. The Aachen Aphasia Test. Adv Neurol 1984; 42: 291-303.
Ille S, Engel L, Kelm A, Meyer B, Krieg SM. Language-Eloquent White Matter Pathway Tractography and the Course of Language Function in Glioma Patients. Front Oncol 2018; 8: 572.
Ille S, Ohlerth AK, Colle D, Colle H, Dragoy O, Goodden J*, et al.* Augmented reality for the virtual dissection of white matter pathways. Acta Neurochir (Wien) 2021; 163(4): 895-903.
Ille S, Sollmann N, Hauck T, Maurer S, Tanigawa N, Obermueller T*, et al.* Impairment of preoperative language mapping by lesion location: a functional magnetic resonance imaging, navigated transcranial magnetic stimulation, and direct cortical stimulation study. J Neurosurg 2015a; 123(2): 314-24.
Ille S, Sollmann N, Hauck T, Maurer S, Tanigawa N, Obermueller T*, et al.* Combined noninvasive language mapping by navigated transcranial magnetic stimulation and functional MRI and its comparison with direct cortical stimulation. J Neurosurg 2015b; 123(1): 212-25.
Isensee F, Schell M, Pflueger I, Brugnara G, Bonekamp D, Neuberger U*, et al.* Automated brain extraction of multisequence MRI using artificial neural networks. Hum Brain Mapp 2019; 40(17): 4952-64.
Jahanshad N, Prasad G, Toga AW, McMahon KL, de Zubicaray GI, Martin NG*, et al.* Genetics of Path Lengths in Brain Connectivity Networks: HARDI-Based Maps in 457 Adults. Multimodal Brain Image Anal (2012) 2012; 7509: 29-40.
Jonasson L, Hagmann P, Bresson X, Thiran JP, Van Wedeen J. Representing diffusion MRI in 5D for segmentation of white matter tracts with a level set method. Inf Process Med Imaging 2005; 19: 311-20.

Kauppi JP, Pajula J, Niemi J, Hari R, Tohka J. Functional brain segmentation using inter-subject correlation in fMRI. Hum Brain Mapp 2017; 38(5): 2643-65.
Kelm A, Sollmann N, Ille S, Meyer B, Ringel F, Krieg SM. Resection of Gliomas with and without Neuropsychological Support during Awake Craniotomy-Effects on Surgery and Clinical Outcome. Front Oncol 2017; 7: 176.
Kocher M, Jockwitz C, Caspers S, Schreiber J, Farrher E, Stoffels G*, et al.* Role of the default mode resting-state network for cognitive functioning in malignant glioma patients following multimodal treatment. Neuroimage Clin 2020; 27: 102287.
Kombos T, Suss O. Neurophysiological basis of direct cortical stimulation and applied neuroanatomy of the motor cortex: a review. Neurosurg Focus 2009; 27(4): E3.
Krause F, Knoblauch A, Brodmann K, Hauptmann A. Die allgemeine chirurgie der gehirnkrankheiten. Stuttgart,: F. Enke; 1914.
Krieg SM, Lioumis P, Makela JP, Wilenius J, Karhu J, Hannula H*, et al.* Protocol for motor and language mapping by navigated TMS in patients and healthy volunteers; workshop report. Acta Neurochir (Wien) 2017; 159(7): 1187-95.
Krieg SM, Picht T, Sollmann N, Bahrend I, Ringel F, Nagarajan SS*, et al.* Resection of Motor Eloquent Metastases Aided by Preoperative nTMS-Based Motor Maps-Comparison of Two Observational Cohorts. Front Oncol 2016; 6: 261.
Krieg SM, Shiban E, Buchmann N, Gempt J, Foerschler A, Meyer B*, et al.* Utility of presurgical navigated transcranial magnetic brain stimulation for the resection of tumors in eloquent motor areas. J Neurosurg 2012; 116(5): 994-1001.
Krieg SM, Tarapore PE, Picht T, Tanigawa N, Houde J, Sollmann N*, et al.* Optimal timing of pulse onset for language mapping with navigated repetitive transcranial magnetic stimulation. Neuroimage 2014; 100: 219-36.
Landgrebe M, Langguth B, Rosengarth K, Braun S, Koch A, Kleinjung T*, et al.* Structural brain changes in tinnitus: grey matter decrease in auditory and non-auditory brain areas. Neuroimage 2009; 46(1): 213-8.
Latora V, Marchiori M. Efficient behavior of small-world networks. Phys Rev Lett 2001; 87(19): 198701.
Lee B, Park JY, Jung WH, Kim HS, Oh JS, Choi CH*, et al.* White matter neuroplastic changes in long-term trained players of the game of "Baduk" (GO): a voxel-based diffusion-tensor imaging study. Neuroimage 2010; 52(1): 9-19.
Lenfeldt N, Larsson A, Nyberg L, Birgander R, Forsgren L. Fractional anisotropy in the substantia nigra in Parkinson's disease: a complex picture. Eur J Neurol 2015; 22(10): 1408-14.
Lerner AJ, Wassermann EM, Tamir DI. Seizures from transcranial magnetic stimulation 2012-2016: Results of a survey of active laboratories and clinics. Clin Neurophysiol 2019; 130(8): 1409-16.
Li Y, Tang C, Lu J, Wu J, Chang EF. Human cortical encoding of pitch in tonal and non-tonal languages. Nat Commun 2021; 12(1): 1161.
Lin D, Wang M, Chen Y, Gong J, Chen L, Shi X*, et al.* Trends in Intracranial Glioma Incidence and Mortality in the United States, 1975-2018. Front Oncol 2021; 11: 748061.
Lioumis P, Zhdanov A, Makela N, Lehtinen H, Wilenius J, Neuvonen T*, et al.* A novel approach for documenting naming errors induced by navigated transcranial magnetic stimulation. Journal of neuroscience methods 2012; 204(2): 349-54.
Llera A, Wolfers T, Mulders P, Beckmann CF. Inter-individual differences in human brain structure and morphology link to variation in demographics and behavior. Elife 2019; 8.
M. Krieg S. Navigated Transcranial Magnetic Stimulation in Neurosurgery. 1st ed. Cham: Springer International Publishing : Imprint: Springer,; 2017. p. 1 online resource (XX, 299 pages 74 illustrations, 65 illustrations in color.
Mitsuhashi T, Sugano H, Asano K, Nakajima T, Nakajima M, Okura H*, et al.* Functional MRI and Structural Connectome Analysis of Language Networks in Japanese-English Bilinguals. Neuroscience 2020; 431: 17-24.
Mole JP, Subramanian L, Bracht T, Morris H, Metzler-Baddeley C, Linden DE. Increased fractional anisotropy in the motor tracts of Parkinson's disease suggests compensatory neuroplasticity or selective neurodegeneration. Eur Radiol 2016; 26(10): 3327-35.

Muhlau M, Rauschecker JP, Oestreicher E, Gaser C, Rottinger M, Wohlschlager AM*, et al.* Structural brain changes in tinnitus. Cereb Cortex 2006; 16(9): 1283-8.
Nahm M, Rousseau D, Greyson B. Discrepancy Between Cerebral Structure and Cognitive Functioning: A Review. J Nerv Ment Dis 2017; 205(12): 967-72.
Negwer C, Beurskens E, Sollmann N, Maurer S, Ille S, Giglhuber K*, et al.* Loss of Subcortical Language Pathways Correlates with Surgery-Related Aphasia in Patients with Brain Tumor: An Investigation via Repetitive Navigated Transcranial Magnetic Stimulation-Based Diffusion Tensor Imaging Fiber Tracking. World Neurosurg 2018; 111: e806-e18.
Negwer C, Sollmann N, Ille S, Hauck T, Maurer S, Kirschke JS*, et al.* Language pathway tracking: comparing nTMS-based DTI fiber tracking with a cubic ROIs-based protocol. J Neurosurg 2017; 126(3): 1006-14.
Norman J. Two visual systems and two theories of perception: An attempt to reconcile the constructivist and ecological approaches. Behav Brain Sci 2002; 25(1): 73-96; discussion -144.
Ogunlade J, Wiginton JGt, Elia C, Odell T, Rao SC. Primary Spinal Astrocytomas: A Literature Review. Cureus 2019; 11(7): e5247.
Ostrom QT, Cioffi G, Gittleman H, Patil N, Waite K, Kruchko C*, et al.* CBTRUS Statistical Report: Primary Brain and Other Central Nervous System Tumors Diagnosed in the United States in 2012-2016. Neuro Oncol 2019; 21(Suppl 5): v1-v100.
Ottenhausen M, Krieg SM, Meyer B, Ringel F. Functional preoperative and intraoperative mapping and monitoring: increasing safety and efficacy in glioma surgery. Neurosurg Focus 2015; 38(1): E3.
Peus D, Newcomb N, Hofer S. Appraisal of the Karnofsky Performance Status and proposal of a simple algorithmic system for its evaluation. BMC Med Inform Decis Mak 2013; 13: 72.
Picht T, Krieg SM, Sollmann N, Rosler J, Niraula B, Neuvonen T*, et al.* A comparison of language mapping by preoperative navigated transcranial magnetic stimulation and direct cortical stimulation during awake surgery. Neurosurgery 2013; 72(5): 808-19.
Plaza M, Gatignol P, Leroy M, Duffau H. Speaking without Broca's area after tumor resection. Neurocase 2009; 15(4): 294-310.
Qiu A, Mori S, Miller MI. Diffusion tensor imaging for understanding brain development in early life. Annu Rev Psychol 2015; 66: 853-76.
Raffa G, Bahrend I, Schneider H, Faust K, Germano A, Vajkoczy P*, et al.* A Novel Technique for Region and Linguistic Specific nTMS-based DTI Fiber Tracking of Language Pathways in Brain Tumor Patients. Front Neurosci 2016; 10: 552.
Ramesh V. Biomolecular and bioanalytical techniques : theory, methodology and applications. Hoboken, NJ: John Wiley & Sons, Inc.,; 2019. p. 1 online resource.
Ratnarajah N, Rifkin-Graboi A, Fortier MV, Chong YS, Kwek K, Saw SM*, et al.* Structural connectivity asymmetry in the neonatal brain. Neuroimage 2013; 75: 187-94.
Ries SK, Dronkers NF, Knight RT. Choosing words: left hemisphere, right hemisphere, or both? Perspective on the lateralization of word retrieval. Ann N Y Acad Sci 2016; 1369(1): 111-31.
Rout MP, Sali A. Principles for Integrative Structural Biology Studies. Cell 2019; 177(6): 1384-403.
Rutter L, Nadar SR, Holroyd T, Carver FW, Apud J, Weinberger DR*, et al.* Graph theoretical analysis of resting magnetoencephalographic functional connectivity networks. Front Comput Neurosci 2013; 7: 93.
Ryali S, Chen T, Padmanabhan A, Cai W, Menon V. Development and validation of consensus clustering-based framework for brain segmentation using resting fMRI. J Neurosci Methods 2015; 240: 128-40.
Sarma RH, Sarma MH. Biological structure and dynamics : proceedings of the ninth Conversation in the Discipline Biomolecular Stereodynamics, held at the State University of New York at Albany, June 20-24, 1995. Schenectady, NY, USA: Adenine Press; 1996.
Schuppert M, Munte TF, Wieringa BM, Altenmuller E. Receptive amusia: evidence for cross-hemispheric neural networks underlying music processing strategies. Brain 2000; 123 Pt 3: 546-59.
Seaquist ER. The Impact of Diabetes on Cerebral Structure and Function. Psychosom Med 2015; 77(6): 616-21.

Seeber M, Cantonas LM, Hoevels M, Sesia T, Visser-Vandewalle V, Michel CM. Subcortical electrophysiological activity is detectable with high-density EEG source imaging. Nat Commun 2019; 10(1): 753.
Seeber M, Michel CM. Synchronous Brain Dynamics Establish Brief States of Communality in Distant Neuronal Populations. eNeuro 2021; 8(3).
Seguin C, van den Heuvel MP, Zalesky A. Navigation of brain networks. Proc Natl Acad Sci U S A 2018; 115(24): 6297-302.
Sollmann N, Fratini A, Zhang H, Zimmer C, Meyer B, Krieg SM. Associations between clinical outcome and tractography based on navigated transcranial magnetic stimulation in patients with language-eloquent brain lesions. J Neurosurg 2019: 1-10.
Sollmann N, Ille S, Hauck T, Maurer S, Negwer C, Zimmer C*, et al.* The impact of preoperative language mapping by repetitive navigated transcranial magnetic stimulation on the clinical course of brain tumor patients. BMC Cancer 2015a; 15: 261.
Sollmann N, Ille S, Obermueller T, Negwer C, Ringel F, Meyer B*, et al.* The impact of repetitive navigated transcranial magnetic stimulation coil positioning and stimulation parameters on human language function. Eur J Med Res 2015b; 20: 47.
Sollmann N, Kelm A, Ille S, Schroder A, Zimmer C, Ringel F*, et al.* Setup presentation and clinical outcome analysis of treating highly language-eloquent gliomas via preoperative navigated transcranial magnetic stimulation and tractography. Neurosurg Focus 2018a; 44(6): E2.
Sollmann N, Negwer C, Tussis L, Hauck T, Ille S, Maurer S*, et al.* Interhemispheric connectivity revealed by diffusion tensor imaging fiber tracking derived from navigated transcranial magnetic stimulation maps as a sign of language function at risk in patients with brain tumors. J Neurosurg 2017; 126(1): 222-33.
Sollmann N, Picht T, Makela JP, Meyer B, Ringel F, Krieg SM. Navigated transcranial magnetic stimulation for preoperative language mapping in a patient with a left frontoopercular glioblastoma. J Neurosurg 2013; 118(1): 175-9.
Sollmann N, Tanigawa N, Ringel F, Zimmer C, Meyer B, Krieg SM. Language and its right-hemispheric distribution in healthy brains: an investigation by repetitive transcranial magnetic stimulation. Neuroimage 2014; 102 Pt 2: 776-88.
Sollmann N, Wildschuetz N, Kelm A, Conway N, Moser T, Bulubas L*, et al.* Associations between clinical outcome and navigated transcranial magnetic stimulation characteristics in patients with motor-eloquent brain lesions: a combined navigated transcranial magnetic stimulation-diffusion tensor imaging fiber tracking approach. J Neurosurg 2018b; 128(3): 800-10.
Sollmann N, Zhang H, Fratini A, Wildschuetz N, Ille S, Schroder A*, et al.* Risk Assessment by Presurgical Tractography Using Navigated TMS Maps in Patients with Highly Motor- or Language-Eloquent Brain Tumors. Cancers (Basel) 2020a; 12(5).
Sollmann N, Zhang H, Kelm A, Schroder A, Meyer B, Pitkanen M*, et al.* Paired-pulse navigated TMS is more effective than single-pulse navigated TMS for mapping upper extremity muscles in brain tumor patients. Clin Neurophysiol 2020b; 131(12): 2887-98.
Song AW, Chang HC, Petty C, Guidon A, Chen NK. Improved delineation of short cortical association fibers and gray/white matter boundary using whole-brain three-dimensional diffusion tensor imaging at submillimeter spatial resolution. Brain Connect 2014; 4(9): 636-40.
Sporns O, Kotter R. Motifs in brain networks. PLoS Biol 2004; 2(11): e369.
Sporns O, Tononi G, Kotter R. The human connectome: A structural description of the human brain. PLoS Comput Biol 2005; 1(4): e42.
Strotzer M. One century of brain mapping using Brodmann areas. Klin Neuroradiol 2009; 19(3): 179-86.
Stultz DJ, Osburn S, Burns T, Pawlowska-Wajswol S, Walton R. Transcranial Magnetic Stimulation (TMS) Safety with Respect to Seizures: A Literature Review. Neuropsychiatr Dis Treat 2020; 16: 2989-3000.
Takarae Y, Zanesco A, Keehn B, Chukoskie L, Muller RA, Townsend J. EEG microstates suggest atypical resting-state network activity in high-functioning children and adolescents with autism spectrum development. Dev Sci 2022: e13231.

Talacchi A, Santini B, Casartelli M, Monti A, Capasso R, Miceli G. Awake surgery between art and science. Part II: language and cognitive mapping. Funct Neurol 2013; 28(3): 223-39.
Tarapore PE, Findlay AM, Honma SM, Mizuiri D, Houde JF, Berger MS*, et al.* Language mapping with navigated repetitive TMS: proof of technique and validation. Neuroimage 2013; 82: 260-72.
Tournier JD, Calamante F, Connelly A. Robust determination of the fibre orientation distribution in diffusion MRI: non-negativity constrained super-resolved spherical deconvolution. Neuroimage 2007; 35(4): 1459-72.
Tuch DS. Q-ball imaging. Magn Reson Med 2004; 52(6): 1358-72.
Tustison NJ, Cook PA, Klein A, Song G, Das SR, Duda JT*, et al.* Large-scale evaluation of ANTs and FreeSurfer cortical thickness measurements. Neuroimage 2014; 99: 166-79.
Tustison NJ, Johnson HJ, Rohlfing T, Klein A, Ghosh SS, Ibanez L*, et al.* Instrumentation bias in the use and evaluation of scientific software: recommendations for reproducible practices in the computational sciences. Front Neurosci 2013; 7: 162.
Uddin S, Khan A, Hossain ME, Moni MA. Comparing different supervised machine learning algorithms for disease prediction. BMC Med Inform Decis Mak 2019; 19(1): 281.
van Straaten EC, Stam CJ. Structure out of chaos: functional brain network analysis with EEG, MEG, and functional MRI. Eur Neuropsychopharmacol 2013; 23(1): 7-18.
Wacker A, Holder M, Will BE, Winkler PA, Ilmberger J. [Comparison of the Aachen Aphasia Test, clinical study and Aachen Aphasia Beside Test in brain tumor patients]. Nervenarzt 2002; 73(8): 765-9.
Wang J, Meng HJ, Ji GJ, Jing Y, Wang HX, Deng XP*, et al.* Finger Tapping Task Activation vs. TMS Hotspot: Different Locations and Networks. Brain Topogr 2020; 33(1): 123-34.
Wang J, Zuo X, He Y. Graph-based network analysis of resting-state functional MRI. Front Syst Neurosci 2010; 4: 16.
Wedeen VJ, Hagmann P, Tseng WY, Reese TG, Weisskoff RM. Mapping complex tissue architecture with diffusion spectrum magnetic resonance imaging. Magn Reson Med 2005; 54(6): 1377-86.
Wolthuis N, Satoer D, Veenstra W, Smits M, Wagemakers M, Vincent A*, et al.* Resting-State Electroencephalography Functional Connectivity Networks Relate to Pre- and Postoperative Language Functioning in Low-Grade Glioma and Meningioma Patients. Front Neurosci 2021; 15: 785969.
Xia M, Wang J, He Y. BrainNet Viewer: a network visualization tool for human brain connectomics. PLoS One 2013; 8(7): e68910.
Yeh FC, Wedeen VJ, Tseng WY. Generalized q-sampling imaging. IEEE Trans Med Imaging 2010; 29(9): 1626-35.
Young JS, Lee AT, Chang EF. A Review of Cortical and Subcortical Stimulation Mapping for Language. Neurosurgery 2021; 89(3): 331-42.
Young RM, Jamshidi A, Davis G, Sherman JH. Current trends in the surgical management and treatment of adult glioblastoma. Ann Transl Med 2015; 3(9): 121.
Yuan B, Zhang N, Yan J, Cheng J, Lu J, Wu J. Tumor grade-related language and control network reorganization in patients with left cerebral glioma. Cortex 2020; 129: 141-57.
Zhang H, Ille S, Sogerer L, Schwendner M, Schroder A, Meyer B*, et al.* Elucidating the structural-functional connectome of language in glioma-induced aphasia using nTMS and DTI. Hum Brain Mapp 2021a.
Zhang H, Schramm S, Schroder A, Zimmer C, Meyer B, Krieg SM*, et al.* Function-Based Tractography of the Language Network Correlates with Aphasia in Patients with Language-Eloquent Glioblastoma. Brain Sci 2020; 10(7).
Zhang N, Li K, Li G, Nataraj R, Wei N. Multiplex Recurrence Network Analysis of Inter-Muscular Coordination During Sustained Grip and Pinch Contractions at Different Force Levels. IEEE Trans Neural Syst Rehabil Eng 2021b; 29: 2055-66.
Zoli M, Talozzi L, Martinoni M, Manners DN, Badaloni F, Testa C*, et al.* From Neurosurgical Planning to Histopathological Brain Tumor Characterization: Potentialities of Arcuate Fasciculus Along-Tract Diffusion Tensor Imaging Tractography Measures. Front Neurol 2021; 12: 633209.